

Incoming Exchange Student - Final Degree Project
Erasmus ☐ Techno ☐ Other (specify):

Degree course: Grau en Enginyeria Química Pla 2009

Title: Metal separation from multi metallic solutions by grape stalks

Document: Final Degree Project

Student (Name & Surname): Bas Stevens

EPS Advisor: Nuria Fiol

Department: Eng. Química, Agrària i Tecn. Agroalimentària

Delivered on (month/year): 01/2016

Metal separation from multi metallic solutions by grape stalks

Bas Stevens

DETAILS PLACEMENT

Period: 14/09/2015 - 22/01/2016

Institute: Universitat de Girona

Lab: Escola Politècnica Superior, MMa

Address: UdG, Escola Politècnica Superior
Ava. Lluís Santalo s/n
17071 Girona, Spain

City: Girona

Country: Spain

Supervisor from host institute: prof. dr. Nuria Fiol and prof.dr. Jordi Poch

Supervisor from Odisee: prof. dr. Patrick Demeyere

Abstract

With the rapid development of various industries such as mine and metallurgy, wastewaters containing metals are directly or indirectly discharged into the environment. One of the most dangerous effluents discharged are Acid Mine Drainage (AMD), the outflows of acidic waters from metal mines. This water needs to be treated so it can be reused and the metal ions in this polluted water can be recuperated.

The metals that occur in the polluted water are difficult to eliminate. To eliminate metals from the water several techniques are used such as chemical precipitation, reverse osmosis or adsorption. In previous research, it has been proven that the sorption process with grape stalks works. Each metal solution behaves differently when sorption takes place. In a metal mixture, this different sorption behaviour could be used for metal ions separation in a metal mixture solution.

The purpose of this work is to separate metals from a multi metallic solution by using grape stalks. The use of sorption process to separate metals from a binary mixture of copper/nickel and cadmium/lead is studied. The sorption process takes place in fixed beds filled with grape stalks. The effect of different parameters such as initial concentration and bed length are studied. Metal concentrations are analysed by flame atomic absorption spectroscopy. The obtained results are presented as breakthrough curves. From these results, the best conditions for metal separation will be established.

Acknowledgements

The city I have chosen was Girona. I had a wonderful time there and met a lot of people who made this journey a lot more fun.

First I would like to thank prof Dr. Nuria Fiol and prof Dr. Jordi Poch who guided me during the project for 5 months. They helped me when help was needed and gave me the right directions during the internship. It wouldn't be possible without them, therefore I am grateful. I also want to thank prof Dr. Florencio de la Torre for his help in the laboratory. Furthermore I would like to thank Odisee for this wonderful experience and in particular my advisor prof Dr. Patrick Demeyere for his feedback and advice before and during the internship.

I would also like to thank my lab partner Nathalie for making the work environment more pleasant.

Special thanks for my parents who convinced me in this great experience and made my stay in Girona possible.

Thank you all for your support, advice and friendship.

Bas Stevens
January 2016

Table of contents

1	INTRODUCTION.....	12
1.1	MINE DRAINAGE.....	12
1.1.1	Occurrence	12
1.1.2	Problems of acid mine drainage (AMD)	12
1.2	THE IBERIAN PYRITE BELT.....	13
1.2.1	The rivers Odiel and Tinto.....	13
1.2.1.1	<i>Values of metal concentrations in the rivers Odiel and Tinto</i>	<i>14</i>
1.3	SOLUTION TO THE PROBLEM OF ACID MINE DRAINAGE.....	15
1.3.1	Treatment technologies for the removal of heavy metals	15
1.3.2	Mechanism of metal sorption	16
1.3.2.1	<i>Description of the sorption process</i>	<i>16</i>
1.3.2.2	<i>Ion exchange.....</i>	<i>16</i>
1.3.2.3	<i>Complexation.....</i>	<i>17</i>
1.3.2.4	<i>Microprecipitation.....</i>	<i>17</i>
1.4	BREAKTHROUGH CURVE	17
1.4.1	Adsorbent.....	17
1.4.2	Breakthrough Curves	18
1.4.3	Calculations	18
1.5	SEPARATION OF THE DIFFERENT METALS DUE TO THE AFFINITY	19
1.5.1	Metal removal by using different columns	19
1.5.2	Metal removal in different metal mixtures	19
1.6	GRAPE STALK	20
1.6.1	Low cost materials as sorbents.....	20
1.6.2	Metal sorption by grape stalk	20
1.6.3	Occurrence and compounds.....	20
1.6.4	The chemical composition of grape stalk.....	21
1.6.4.1	<i>Cellulose.....</i>	<i>21</i>
1.6.4.2	<i>Hemicelluloses.....</i>	<i>21</i>
1.6.4.3	<i>Tannin</i>	<i>21</i>
1.6.4.4	<i>Polyphenols.....</i>	<i>22</i>
1.6.4.5	<i>Lignin.....</i>	<i>22</i>
1.7	FAAS	23
1.7.1	Instrumental set-up.....	23

1.7.2	Instrument components.....	23
1.7.2.1	Hollow cathode lamp.....	23
1.7.2.2	Burners	24
1.7.2.3	Flame.....	24
1.7.2.4	Monochromator	25
1.7.2.5	Readout component.....	25
2	OBJECTIVES.....	26
3	EXPERIMENTAL PART	27
3.1	MATERIALS AND METHODS.....	27
3.1.1	Grape stalks.....	27
3.1.1.1	Occurrence	27
3.1.1.2	Grape stalks preparation.....	27
3.1.1.3	Preparation of the column	28
3.1.2	Experimental set-up	28
3.1.3	Flow rate	28
3.1.4	Analysis of the metals.....	28
3.1.4.1	FAAS.....	28
3.1.4.2	Lamps.....	29
3.1.4.3	Automatic dilutor	29
3.1.5	Stock solutions.....	29
3.1.5.1	Copper	29
3.1.5.2	Nickel.....	29
3.1.5.3	Lead.....	29
3.1.5.4	Cadmium.....	30
3.1.6	preparation of the columns	30
3.1.7	Metal mixtures	31
3.1.7.1	Heavy metal solutions	31
3.1.7.2	Calculations of metal mixture 1 of Cu and Ni.....	31
3.1.7.3	Calculations of metal mixture 6 of Pb and Cd.....	32
4	RESULTS.....	33
4.1	EFFECT OF THE BED LENGTH	33
4.1.1	Experiments of Copper and nickel with different bed length	33
4.1.1.1	Binary mixture of Cu/Ni with a full column (2 g of grape stalks).....	33
4.1.1.2	Binary mixture of Cu/Ni with a half filled column (1 g of grape stalks).....	34
4.1.1.3	Binary mixture of Cu/Ni with a quarter filled column (0,5 g of grape stalks).....	36

4.1.1.4	<i>Summary of the study of the bed length with copper and nickel</i>	38
4.1.2	Experiments with Cadmium and lead with different bed length.....	38
4.1.2.1	<i>Binary mixture of Cd/Pb with a full column (2 g of grape stalks)</i>	38
4.1.2.2	<i>Binary mixture of Cd/Pb with a half filled column (1 g of grape stalks)</i>	39
4.1.2.3	<i>Binary mixture of Cd/Pb with a quarter filled column (0,5 g of grape stalks)</i>	40
4.1.2.4	<i>Summary of the study of the bed length with lead and cadmium</i>	41
4.2	EFFECT OF METAL CONCENTRATIONS	42
4.2.1	Concentration ratio's of Copper and Nickel	42
4.2.1.1	<i>Binary metal mixture of 5,4 mg/L copper and 145 mg/L nickel.....</i>	42
4.2.1.2	<i>Binary metal mixture of 14,5 mg/L copper and 145 mg/L nickel.....</i>	43
4.2.1.3	<i>Binary metal mixture of 35 mg/L copper and 145 mg/L nickel.....</i>	43
4.2.1.4	<i>Binary metal mixture of 72,5 mg/L copper and 145 mg/L nickel.....</i>	44
4.2.1.5	<i>Binary metal mixture of 145 mg/L copper and 145 mg/L nickel.....</i>	45
4.2.1.6	<i>Relationship between the separation volume and the initial concentration of copper.....</i>	46
4.2.2	Concentration ratio's of lead and cadmium.....	46
4.2.2.1	<i>Binary metal mixture of 3 mg/L lead and 40 mg/L cadmium</i>	46
4.2.2.2	<i>Binary metal mixture of 9 mg/L lead and 40 mg/L cadmium</i>	47
4.2.2.3	<i>Binary metal mixture of 20 mg/L lead and 40 mg/L cadmium</i>	47
4.2.2.4	<i>Binary metal mixture of 40 mg/L lead and 40 mg/L cadmium</i>	48
4.2.2.5	<i>Relationship between the separation volume and the initial concentration of lead ..</i>	49
4.3	BED-DEPTH SERVICE TIME MODEL (BDST)	49
4.3.1	Relationship between the separation time and the bed length for the binary metal mixture of copper and nickel.....	50
4.3.2	Relationship between the separation time and the bed length for the binary metal mixture of cadmium and lead.....	51
5	CONCLUSIONS	53
6	ANNEX.....	54
7	BIBLIOGRAPHY.....	55

List of figures

Figure 1: Diagram of acid mine drainage (http://ca.water.usgs.gov/projects/iron_mountain/environment.html)	12
Figure 2: Diagrammatic block showing the Tinto-Odiel river and the estuary system (Galán, et al., 2001)	13
Figure 3: River Tinto (https://en.wikipedia.org/wiki/Acid_mine_drainage)	13
Figure 4: River Odiel (http://www.eldiario.es/andalucia/enclave_rural/Expertos-Universidad-Huelva-depurar-contaminada_0_284172244.html)	13
Figure 5: Sketch map of the Tinto and Odiel rivers, stream gauging stations, rain gauges, and main mine localities. (Galán, et al., 2001)	14
Figure 6: Adsorption process (Volesky, 2003)	16
Figure 7: Ion exchange steps (Volesky, 2003)	16
Figure 8: Complexation of copper (Volesky, 2003)	17
Figure 9: Micro precipitation process (Volesky, 2003)	17
Figure 10: Figure of the mass transfer zone (http://facstaff.cbu.edu/rprice/lectures/adsorb.html)	18
Figure 11: Typical breakthrough curve (http://facstaff.cbu.edu/rprice/lectures/adsorb.html)	18
Figure 12: Grape stalk.....	21
Figure 13: Structure of cellulose (http://www.homeopathie-equilibrium.nl/Lists/Berichten/Post.aspx?ID=89).....	21
Figure 14: Structure of hemicelluloses (https://en.wikipedia.org/wiki/Hemicellulose)	21
Figure 15: Structure of flavone (http://www.chemsynthesis.com/base/chemical-structure-7141.html)	22
Figure 16: Structure of gallic acid (http://www.guidchem.com/reference/dic-3209.html)	22
Figure 17: Structure of Phloroglucinol (http://www.wikiwand.com/nl/Floroglucinol)	22
Figure 18: Chemical structure of lignin (https://en.wikipedia.org/wiki/Lignin)	22
Figure 19: Sketch of the components of the FAAS (http://faculty.sdmiramar.edu/fgarces/labmatters/instruments/aa/AAS_Theory/AASTheory.htm)	23
Figure 20: Illustration of the method of the hollow cathode lamp (http://faculty.sdmiramar.edu/fgarces/labmatters/instruments/aa/AAS_Theory/AASTheory.htm)	23
Figure 21: The nebulizer (http://faculty.sdmiramar.edu/fgarces/labmatters/instruments/aa/AAS_Theory/AASTheory.htm)	24
Figure 22: The premix burner (http://faculty.sdmiramar.edu/fgarces/labmatters/instruments/aa/AAS_Theory/AASTheory.htm)	24
Figure 23: Vineyard in the Costa Brava (northern Spain)	27
Figure 24: Grinder (Pro prop cuisine art)	27
Figure 25: Parts of interest of grape stalks	27
Figure 26: Automatic siever (CISA)	27
Figure 27: Sieved grape stalks with a particle size between 250 and 500 μm	27
Figure 28: Glass wool.....	28
Figure 29: Fixed bed filled with grape stalks	28
Figure 30: Experimental set-up.....	28
Figure 31: Breakthrough curve of copper with a full column (conditions: $C_{i, \text{cu}} = 5,78 \text{ mg/L}$; $C_{i, \text{ni}} = 155 \text{ mg/L}$; column length = 7 cm)	33
Figure 32: Breakthrough curve of nickel with a full column (conditions: $C_{i, \text{cu}} = 5,78 \text{ mg/L}$; $C_{i, \text{ni}} = 155 \text{ mg/L}$; column length = 7 cm.....	33
Figure 33: Breakthrough curve of copper and nickel with a full column (conditions: $C_{i, \text{cu}} = 5,78 \text{ mg/L}$; $C_{i, \text{ni}} = 155 \text{ mg/L}$; column length = 7 cm; flow rate = 30 ml/hour).....	34
Figure 34: Breakthrough curve of copper with a half filled column (conditions: $C_{i, \text{cu}} = 5,25 \text{ mg/L}$; $C_{i, \text{ni}} = 131,04 \text{ mg/L}$; column length = 3,5 cm).....	35
Figure 35: Breakthrough curve of nickel with a half filled column (conditions: $C_{i, \text{cu}} = 5,25 \text{ mg/L}$; $C_{i, \text{ni}} = 131,04 \text{ mg/L}$; column length = 3,5 cm)	35

Figure 36: Breakthrough curve of copper and nickel with a half filled column (conditions: $C_{i, cu} = 5,25$ mg/L; $C_{i, ni} = 131,04$ mg/L; column length = 3,5 cm; flow rate = 30 ml/hour)	36
Figure 37: Breakthrough curve of copper with a column filled with 0,5 g of grape stalks (conditions: $C_{i, cu} = 4,95$ mg/L; $C_{i, ni} = 160,0$ mg/L; column length = 1,75 cm)	36
Figure 38: Breakthrough curve of nickel with a column filled with 0,5 g of grape stalks (conditions: $C_{i, cu} = 4,95$ mg/L; $C_{i, ni} = 160,0$ mg/L; column length = 1,75 cm)	37
Figure 39: Breakthrough curve of copper and nickel with a column filled with 0,5 g of grape stalks (conditions: $C_{i, cu} = 4,95$ mg/L; $C_{i, ni} = 160,0$ mg/L; column length = 1,75 cm; flow rate = 30 ml/hour)	37
Figure 40: Breakthrough curve of lead and cadmium with a full column (conditions: $C_{i, pb} = 40,38$ mg/L; $C_{i, cd} = 47,67$ mg/L; column length = 7 cm; flow rate = 30 ml/hour)	38
Figure 41: Breakthrough curve of lead and cadmium with a full column (conditions: $C_{i, pb} = 40,38$ mg/L; $C_{i, cd} = 47,67$ mg/L; column length = 7 cm; flow rate = 30 ml/hour)	39
Figure 42: Breakthrough curve of Pb and Cd with a half filled column (conditions: $C_{i, pb} = 40,93$ mg/L; $C_{i, cd} = 45,71$ mg/L; column length = 3,5 cm; flow rate = 30 ml/hour)	39
Figure 43: Breakthrough curve of Pb and Cd with a half filled column (conditions: $C_{i, pb} = 40,93$ mg/L; $C_{i, cd} = 45,71$ mg/L; column length = 3,5 cm; flow rate = 30 ml/hour)	40
Figure 44: Breakthrough curve of Pb and Cd with a column filled with 0,5 g of grape stalks	40
Figure 45: Breakthrough curve of Pb and Cd with a column filled with 0,5 g of grape stalks	41
Figure 46: Breakthrough curve of copper and nickel with a full column (conditions: $C_{i, cu} = 5,78$ mg/L; $C_{i, ni} = 155$ mg/L; column length = 7 cm; flow rate = 30 ml/hour)	42
Figure 47: Breakthrough curve of 14,5 mg/L copper in a binary mixture of copper and nickel (conditions: $C_{i, cu} = 14,92$ mg/L; $C_{i, ni} = 145,84$ mg/L; column length = 7 cm; flow rate = 30 ml/hour)	43
Figure 48: Breakthrough curve of 35 mg/L copper in a binary mixture of copper and nickel (conditions: $C_{i, cu} = 38,84$ mg/L; $C_{i, ni} = 142,77$ mg/L; column length = 7 cm; flow rate = 30 ml/hour)	44
Figure 49: Breakthrough curve of 72,5 mg/L copper in a binary mixture of copper and nickel (conditions: $C_{i, cu} = 74,55$ mg/L; $C_{i, ni} = 154,12$ mg/L; column length = 7 cm; flow rate = 30 ml/hour)	44
Figure 50: Breakthrough curve of 145 mg/L copper in a binary mixture of copper and nickel (conditions: $C_{i, cu} = 153,24$ mg/L; $C_{i, ni} = 158,14$ mg/L; column length = 7 cm; flow rate = 30 ml/hour)	45
Figure 51: Relationship between the separation volume and the initial concentration of copper	46
Figure 52: Breakthrough curve of 3 mg/L lead in a binary mixture of lead and cadmium (conditions: $C_{i, pb} = 3,18$ mg/L; $C_{i, cd} = 42,68$ mg/L; column length = 7 cm; flow rate = 30 ml/hour)	46
Figure 53: Breakthrough curve of 9 mg/L lead in a binary mixture of lead and cadmium (conditions: $C_{i, pb} = 8,88$ mg/L; $C_{i, cd} = 41,68$ mg/L; column length = 7 cm; flow rate = 30 ml/hour)	47
Figure 54: Breakthrough curve of 20 mg/L lead in a binary mixture of lead and cadmium (conditions: $C_{i, pb} = 18,24$ mg/L; $C_{i, cd} = 42,05$ mg/L; column length = 7 cm; flow rate = 30 ml/hour)	47
Figure 55: Breakthrough curve of Pb and Cd with a full column (conditions: $C_{i, pb} = 40,38$ mg/L; $C_{i, cd} = 47,67$ mg/L; column length = 7 cm; flow rate = 30 ml/hour)	48
Figure 56: Relationship between the separation volume and the initial concentration of lead	49
Figure 57: Relationship between the separation time and the bed length of the binary metal mixture of copper and nickel	50
Figure 58: Relationship between the separation time and the bed length of the binary metal mixture of lead and cadmium	51

List of tables

Table 1: Concentration ranges of heavy metals in the river Odiel	14
Table 2: Heavy metal concentration ranges in the river Tinto (José, et al., 2006)	15
Table 3: Summary of the study of the bed length	30
Table 4: Concentration of the metals used in the binary metal mixtures.....	31
Table 5: Summary of the study of the bed length of copper and nickel	38
Table 6: Summary of the study of the bed length of lead and cadmium	41
Table 7: Concentrations ranges used in the binary metal mixtures.....	42
Table 8: Summary of the separation volume of the binary metal mixture as a function of copper concentration at a fixed nickel concentration of 145 mg/L.....	45
Table 9: Summary of the concentration ranges of the binary metal mixture of lead and cadmium	48
Table 10: N_0 and K values for copper	50
Table 11: Prediction of the BDST for the metal mixture of copper/nickel for different copper concentrations	50
Table 12: Prediction of the BDST for the metal mixture of copper 5,4 mg/L and nickel 145 mg/L for different bed lengths	51
Table 13: N_0 and K values for lead	52
Table 14: Prediction of the BDST for the metal mixture of lead/cadmium for different lead concentrations	52
Table 15: Prediction of the BDST for the metal mixture of lead 45 mg/L and cadmium 52 mg/L for different bed lengths	52
Table 16: pump tubes color codes	54

1 INTRODUCTION

1.1 MINE DRAINAGE

1.1.1 Occurrence

Mine drainage is formed by metal-rich water from chemical reaction between water and rocks containing sulphur-bearing metals. The acidic water frequently comes from areas where mine activities have exposed rocks containing pyrite. The iron that is exposed in the water by mine drainage can form red, orange or yellow sediments in the bottom of streams. But also other metals get exposed by acid drainage such as aluminium, chromium, nickel, cadmium, lead, ... (Sweeney, 1992)

1.1.2 Problems of acid mine drainage (AMD)

Acid mine drainage (AMD) is a serious water pollution problem. The outflow of acidic waters due to the metal mines can cause a big ecological and economic impact on the environment and living beings. Acid mine drainage is responsible for the pollution and degraded water quality in groundwater, streams and rivers. Moreover, fish species decline in outdoor recreation and tourism along with contamination of groundwater drinking supplies. In southern Spain there is an area where acid mines are causing those problems. Some of these acid mines are located in the Iberian Pyrite Belt (Ayora, et al., 2012). Figure 1 represents the process of acid mine drainage at an iron mountain mine. Rainfall runs off the surface of the mountain and drains through the mountain pit. The rain is responsible for the entrainment of the heavy metals that are present in the mines.

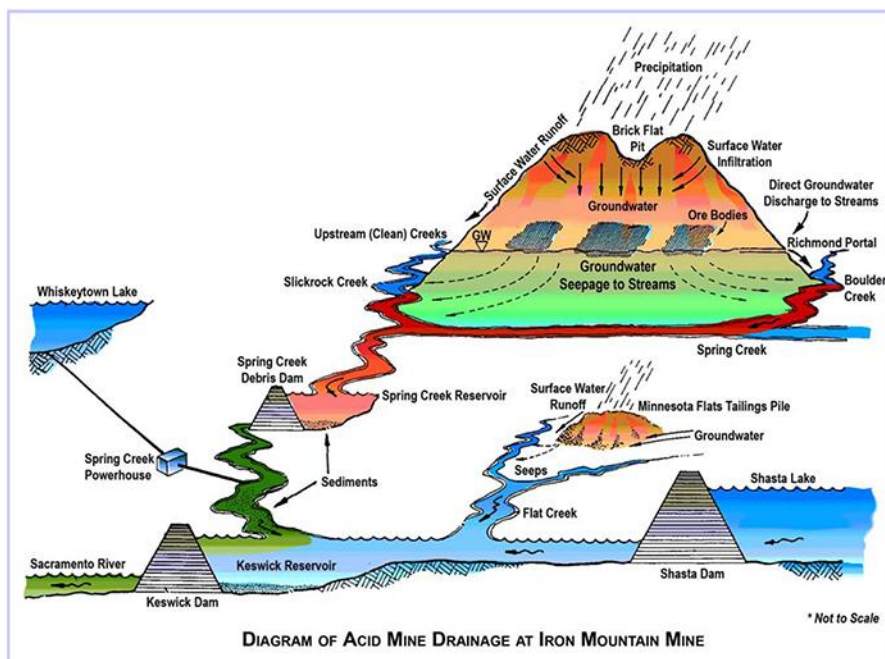


Figure 1: Diagram of acid mine drainage

(http://ca.water.usgs.gov/projects/iron_mountain/environment.html)

1.2 THE IBERIAN PYRITE BELT

The Iberian Pyrite Belt is one of the largest metallogenic sulphide deposits in the world. Intensive mining and melting activities in the Iberian pyrite belt occurred since the mid- 19th century, particularly in the Rio Tinto mining district. A lot of abandoned mine sites of the Iberian pyrite belt are drained, in its Spanish extension, by the Odiel and Tinto rivers. (Galán, et al., 2001)

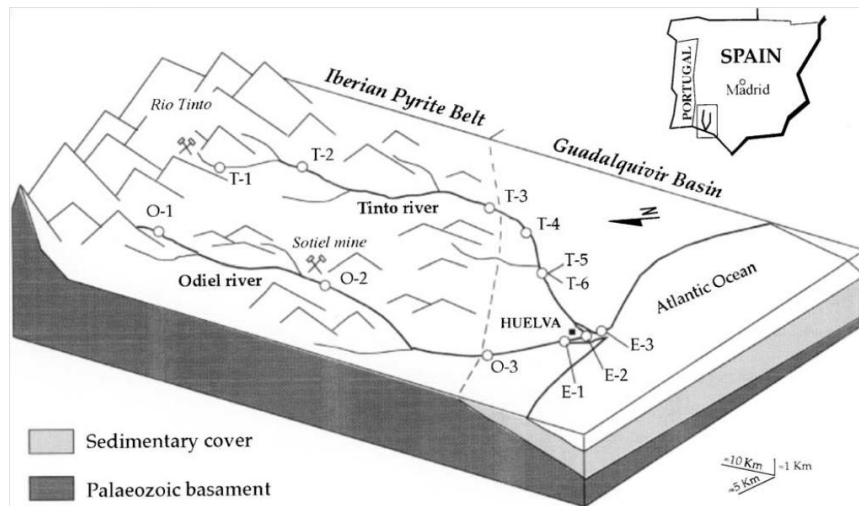


Figure 2: Diagrammatic block showing the Tinto-Odiel river and the estuary system (Galán, et al., 2001)

1.2.1 The rivers Odiel and Tinto

The Odiel river comes from Sierra de Aracena and the Tinto river from Peña del Hierro mine. Both rivers meet in a common estuary, known as the Ria of Huelva. The Tinto River has a length of approximately 100 km and has a surface of the watershed of 720 km². The Odiel river has a length of approximately 140 km long and its surface of its drainage basin is 2 300 km². Both rivers show a typical red-wine colour and are characterised by pH values from 2 to 4, within the range normally reported for acid mine drainage. (Nieto, et al., 2013)



Figure 3: River Tinto

(https://en.wikipedia.org/wiki/Acid_mine_drainage)



Figure 4: River Odiel

(http://www.eldiario.es/andalucia/enclave_rural/Expertos-Universidad-Huelva-depurar-contaminada_0_284172244.html)

The metal concentrations in the two rivers due to the acidic outflow of the metal mines have been investigated. (Ayora, et al., 2012)

1.2.1.1 Values of metal concentrations in the rivers Odiel and Tinto

The concentration levels of some heavy metals that occurred in the rivers Odiel and Tinto can be found in table 1. The results of the concentration levels of the metals were obtained by taking water samples on several locations along the rivers. The sketch map below shows the sampling points where the water samples were taken. (Galán, et al., 2001)

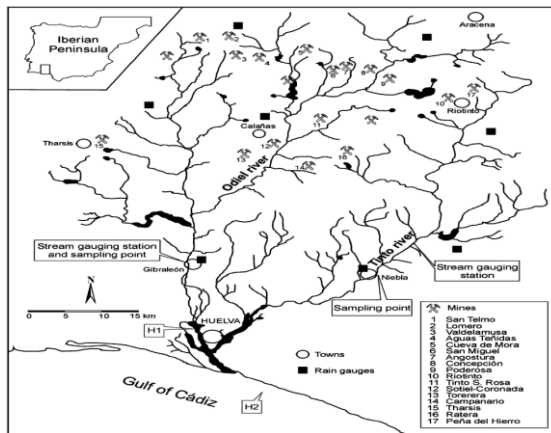


Figure 5: Sketch map of the Tinto and Odiel rivers, stream gauging stations, rain gauges, and main mine localities. (Galán, et al., 2001)

a) Metal concentration in the river Odiel

Some of the metal concentrations that were found in the river Odiel are presented in table 1.

Table 1: Concentration ranges of heavy metals in the river Odiel (José, et al., 2006)

Metals (mg/L)	Mean (mg/L)	Min (mg/L)	Max (mg/L)
Ca	45,7	11,9	161,0
Mg	70,5	10,1	224,1
Na	17,3	7,9	32,7
K	2,4	0,2	37,3
Al	32,8	0,58	175,8
Fe	4,9	0,31	23,5
Cu	5,4	0,5	17,1
Mn	8,1	0,9	32,1
Zn	11,5	1,3	36,4
As (µg/L)	4	<3	22
Ba (µg/L)	21	<1	42
Cd	52	5	176
Ni	145	19	500
Pb	45	<7	267

b) Metal concentration in the river Tinto

Some of the metal concentrations that were found in the river Tinto are presented in table 2.

Table 2: Heavy metal concentration ranges in the river Tinto (José, et al., 2006)

Metal	Tinto River	
	Min (mg/L)	Max (mg/L)
Al	18,0	2,88
As	Bdl	0,0452
Ca	10,9	458
Cd (µg/L)	Bdl	0,00291
Co (µg/L)	0,0242	0,142
Cr (µg/L)	Bdl	0,826
Cu	4,80	379
Fe	7,60	28,3
K	0,100	31,0
Mg	2,35	24,0
Mn	2,20	188
Na	2,09	196
Ni	0,00269	0,0470
Pb	Bdl	0,00272
Si	5,70	73,1
Zn	4,60	317

Bdl: below detection limit

1.3 SOLUTION TO THE PROBLEM OF ACID MINE DRAINAGE

1.3.1 Treatment technologies for the removal of heavy metals

A wide variety of treatment technologies have been investigated and developed for the decontamination of metal-polluted effluents. A summary of the treatments: chemical precipitation, ion exchange, solvent extraction, membrane processes, electrochemical techniques and adsorption. Adsorption is a process by which molecules adhere to solid surfaces. The attraction may often be based on electrostatic charges. Negative adsorption is the adsorption of positive species on negative adsorption sites and vice versa for positive adsorption. While the term adsorption implies a surface phenomenon, the actual sequestration may take place based on either physical phenomena (physical adsorption) or through a variety of chemical binding means (chemisorptions). There are also possible oxidation/reduction reactions taking place in the sorbent. It is quite possible that at least some of these mechanisms are acting simultaneously to varying degrees depending on the sorbent and the solution environment. (Oñate, 2009)

The problems of acid mine drainage can be solved by using biomaterials as sorbents to remove heavy metals from the drained water. These biomaterials are called biosorbents and are derived from raw microbial, seaweed or some plant biomass through different kinds of simple procedures. Biosorbents are capable of directly sorbing metal ionic species from aqueous solutions. Biosorbents are used to adsorb the metals out of the water by different mechanisms that will be explained later.

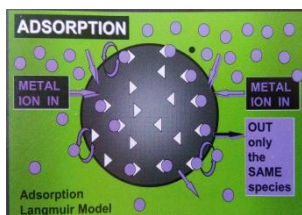


Figure 6: Adsorption process (Volesky, 2003)

1.3.2 Mechanism of metal sorption

1.3.2.1 Description of the sorption process

Sorption is the process of accumulation in an interface of substances that initially were in solution. The adsorbent is the solid, liquid or gas phase in which the sorbent is being accumulated and the adsorbate is the substance that is being removed from the fluid.

Sorption takes place in four steps: (1) solute transport from the bulk of the solution, (2) diffusion through the fluid film that surrounds the particle to the surface, (3) intraparticle diffusion and (4) adsorption. Sorption can be distinguished in two different terms: adsorption and absorption. Absorption involves the concentration of the absorbate in the whole volume of the sorbent, while adsorption involves the accumulation or concentration of the sorbed substance in the surface.

The most remarkable forces responsible for sorption are:

- Dipole-dipole and Coulombic interactions
- London or Van der Waals forces
- Covalent bonds
- Hydrogen bridges

A number of different mechanisms have been postulated to be active in biosorption such as:

- Chemisorptions by ion exchange, complexation, coordination, chelation;
- Physical adsorption and microprecipitation.

1.3.2.2 Ion exchange

Ion exchange is the interchange of ions which are formed by molecular or atomic species either losing or gaining electrons. The ion exchange properties of certain natural polysaccharides have been studied in detail and it is well established that bivalent metal ions exchange with counter-ions from active groups of polysaccharides. The most important mechanism during this sorption process is ion exchange.

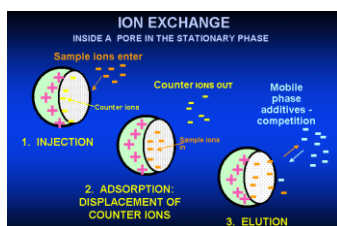


Figure 7: Ion exchange steps (Volesky, 2003)

1.3.2.3 Complexation

complexation is defined as the formation of a species by the association of two or more species. When one of the species is a metal ion, the resulting entity is known as a metal complex. Mononuclear complexes are formed between a metal ion and a number of anion, or ligands. There are complexes which contain more than one metal atom center. A more elaborate example of complexation is shown in the figure below. (Volesky, 2003)

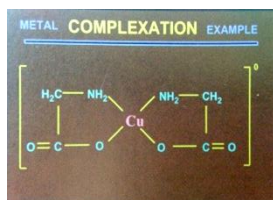


Figure 8: Complexation of copper (Volesky, 2003)

1.3.2.4 Microprecipitation

Microprecipitation of metals results when the solubility of the sorbate reaches its limit. This may happen even due to local conditions, not necessarily in the bulk of the solution. With micro precipitation the sorbate is deposited in clusters and filtration may gain predominance. (Volesky, 2003)

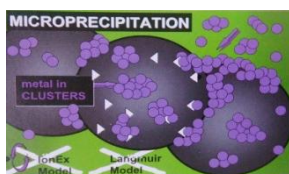


Figure 9: Micro precipitation process (Volesky, 2003)

1.4 BREAKTHROUGH CURVE

1.4.1 Adsorbent

A component can be separated from a mixture if it selectively adsorbs onto a solid surface. Adsorbents are usually porous solids and adsorption occurs mainly on the pore walls inside particles. Some examples of adsorbents include: activated carbon, silica gel, zeolites, synthetic resins, coffee waste and grape stalk. Fluid flows up through the bed and the metals adsorb onto the solid. Different steps of the sorption process can be summarized:

1. Solute diffuses through the fluid to an area near the solid particle surface.
2. Solute diffuses into the pores of the particle.
3. Solute diffuses to the pore wall.
4. Solute adsorbs to the pore wall surface.

1.4.2 Breakthrough Curves

The amount of material adsorbed within a bed depends both on position and time. As fluid enters the bed, it comes in contact with the first few layers of absorbent. Solute adsorbs, filling up some of the available sites. Then, the adsorbent near the entrance is saturated and the fluid penetrates farther into the bed before all solute is removed. Thus the active region shifts up through the bed as time goes on. The first drops of the fluid emerging from the bed will have little or no solute remaining, until the bulk of the bed becomes saturated. The breakthrough point occurs when the concentration of the fluid leaving the bed spikes as unabsorbed solute begins to emerge. At this point, the bed has become ineffective. As the concentration wave moves through the bed, most of the mass transfer is occurring in a rather small region. This mass transfer zone moves up the bed until it breaks through. The shape of the mass transfer zone depends on the adsorption isotherm, flow rate and the diffusion characteristics.

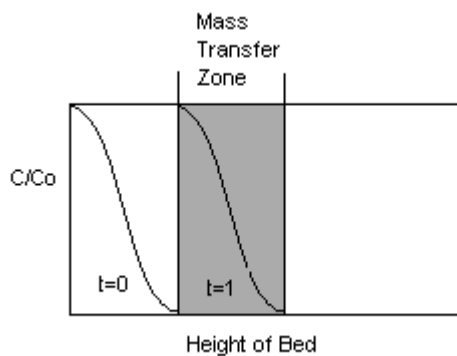


Figure 10: Figure of the mass transfer zone (<http://facstaff.cbu.edu/rprice/lectures/adsorb.html>)

The wave front may change shape as it moves through the bed. In figure 11 an example of a breakthrough curve is presented. The breakthrough curve presents an S-shape. During the elapsed time the concentration of the solution that emerged from the column is zero until the concentration starts to increase because the sorbent is getting saturated. The sorbent is ineffective when the sorbent is saturated.

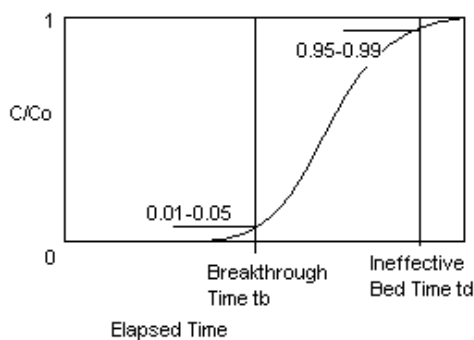


Figure 11: Typical breakthrough curve (<http://facstaff.cbu.edu/rprice/lectures/adsorb.html>)

1.4.3 Calculations

When scaling up an adsorber, the key design parameter is the length of the bed. The total length is split into the "required length" of an "ideal" fixed bed process and a segment of "unused bed" that is

the length leftover at breakthrough. By adding these together, you obtain a bed that can achieve the needed removal, but not waste solute.

The diameter of the bed is calculated from the fluid flow rate and the desired cycle time. Usually, superficial velocities on the order of 0.15 to 0.45 m/s are targeted.

Capacity calculations are made based on plots of the composition vs. time (usually near the exit of the bed). Curves are integrated (analytically, numerically, or graphically) to obtain capacities (measured in time units, or how long a bed can run). In this work, the curves are integrated graphically to calculate the capacity of the sorbent.

1.5 SEPARATION OF THE DIFFERENT METALS DUE TO THE AFFINITY

1.5.1 Metal removal by using different columns

Sorbent bed height strongly affects the volume of the solution treated or throughput volume. The breakthrough curves are following a characteristic S-shape profile, which is associated with an adsorbate of smaller molecular diameter and more simple structure. An increase in column depth increases the treated volume due to a high contact time. The exhaust time increases with increasing bed height, as more binding sites were available for sorption. The increase in adsorbent with bed depth is due to the increase in adsorbent doses which provides greater adsorption sites. (Negrea, et al., 2011)

1.5.2 Metal removal in different metal mixtures

When the column capacity is approached, species with a lower affinity are pushed off by others with higher affinity and displacement of the first species occurs (Trujillo, et al., 1991; Kratochvil and Volesky, 1998). In previous works, metal elimination of divalent metals in mixtures by sorption onto grape stalks performed in fixed bed columns was studied. It was observed that, from four metallic ions (Cu, Ni, Cd and Pb) in binary mixtures, both metals were sorbed by grape stalks. Some metals have a higher affinity to be sorbed onto grape stalks. Because of this different affinity, one metal initially sorbed, was replaced by a second metal with higher affinity. This replacement was observed as an overconcentration in an outlet solution. An important result of this work was that only Pb(II) did not suffer overconcentration. This fact suggests that the affinity of grape stalks for Pb(II) has to be greater than for the other three metals. Also, it was observed that Cu(II) was only overshoot in binary mixtures when the solution contained Pb(II), so that, the affinity Cu(II)-grape stalks should be lower than Pb(II)-grape stalks but higher than Ni(II)-grape stalks and Cd(II)-grape stalks. Of course it's clear that Ni(II) and Cd(II) would overshoot in presence of Pb(II). Finally, to determine which of these two metals, Ni(II) and Cd(II) would exhibit the weakest interaction with grape stalks, its sorption behaviour in the binary mixture Ni(II) -Cd(II) was analyzed. Ni(II) suffered a slight overshoot, indicating thus that, despite the affinity of GS for Ni(II) would be lower than for Cd(II), the difference does not have to be so high. According to the results obtained and discussed, an affinity ranking for the sorption of the different divalent cations onto grape stalks was proposed. This ranking is, from higher to lower sorbent affinity: $Pb > Cu > Cd > Ni$. (Oñate, 2009). These difference in sorption affinity could allow us to use the biosorption process onto grape stalks to separate these metals ions from binary metal mixtures solutions.

1.6 GRAPE STALK

1.6.1 Low cost materials as sorbents

A wide variety of materials that are fully available have been employed sorbents such as natural, agricultural or industrial by-products. These materials are mainly natural or agricultural wastes but also industrial wastes or process by-products. The main attractive of the use of this kind of technology is based on two aspects. The first one is the intrinsic low cost of the materials. The second is that in the case of reuse of industrial by-products, an added value is conferred to these materials. Otherwise they would be considered as wastes, raising the costs in the industry, because they have to be transported to the agreed centres for treatment, management or disposal.

These materials can be used either on its raw form or after a previous treatment to enhance their sorption capacity or to improve their mechanical or mass transfer properties. One of those low-cost materials are grape stalks. (Pujol, et al., 2013)

1.6.2 Metal sorption by grape stalk

The removal of metals from binary metal mixtures of Cu (II) and Ni (II) and Cd (II) and Pb (II) by using grape stalks was investigated in earlier works (Villaescusa et al., 2004). Metals can be distinguished from other toxic pollutants, since they are not biodegradable and can be accumulated in living tissues. Activated carbon is often used in adsorption processes but is too expensive so the alternatives that are used are low-cost sorbing materials such as grape stalks for the removal of heavy metals. The sorption of metals by this kind of material might be due to the presence of carboxyl, hydroxyl, sulphate, phosphate and amino groups that can bind metal ions. (Pujol, et al., 2013)

1.6.3 Occurrence and compounds

Grape stalks are the grape lignocellulosic skeleton of grapes that are obtained from stripping operations during processing. Stalks represent between 2,5 % and 7,5 % of the weight of the grapes. Catalonia is an important wine producing region in the Mediterranean area located in the north-east coast of Spain. In one year more than 10 000 tons of grape stalks is left as waste. These wastes are not hazardous but they have to be landfill disposed, incinerated or biologically treated and therefore causing an economical and environmental problem.

Grape stalks waste has been investigated as a source of cellulose and hemicelluloses (Spigno et al., 2008), natural antioxidants by the extraction of phenolic compounds (Garcia-Perez et al., 2010; Makris et al., 2007; Spigno and DeFaveri, 2007), fermentable sugars via enzymatic treatment for biofuel production (Mazzaferro et al., 2011). The main components of grape stalks are extractives, especially polar extractives soluble in hot water and in alkali, with a high content in tannins and other polyphenolic compounds. Then there are structural components (lignin and polysaccharides). The chemical nature of the surface of grape stalks is very important. It makes it an universal adsorbent to remove a great variety of substances. (Pujol, et al., 2013)



Figure 12: Grape stalk

1.6.4 The chemical composition of grape stalk

1.6.4.1 Cellulose

Cellulose is a natural polysaccharide produced by linking additional sugars of B-D glucose in exactly the same way. The sugar units are linked when water is eliminated by combining the –OH Group and H. The length of the chain varies greatly, from a few hundred sugar units to over 6000.

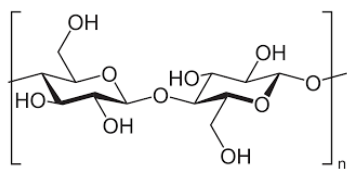


Figure 13: Structure of cellulose (<http://www.homeopathie-equilibrium.nl/Lists/Berichten/Post.aspx?ID=89>)

1.6.4.2 Hemicelluloses

A hemicelluloses is any of several heteropolymers, present along with cellulose in almost all plant cell walls. Hemicelluloses has a random, amorphous structure with little strength.

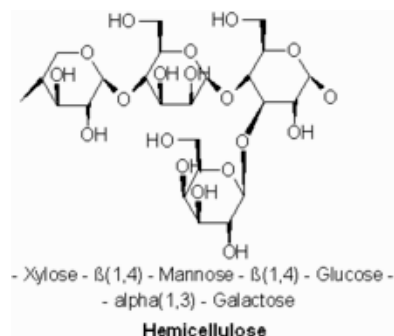
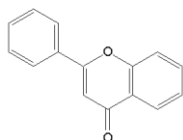


Figure 14: Structure of hemicelluloses (<https://en.wikipedia.org/wiki/Hemicellulose>)

1.6.4.3 Tannin

A tannin is a type of bio molecule, a bitter plant polyphenolic compound that binds to and precipitates proteins and various other organic compounds including amino acids and alkaloids. An example of a tannin is presented in figure 9.

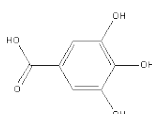


Flavone:

Figure 15: Structure of flavone (<http://www.chemsynthesis.com/base/chemical-structure-7141.html>)

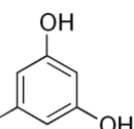
1.6.4.4 Polyphenols

Polyphenols are a structural class of mainly natural, but also synthetic or semisynthetic organic chemicals characterized by the presence of large multiples of phenolstructural units.



- Gallic acid:

Figure 16: Structure of gallic acid (<http://www.guidchem.com/reference/dic-3209.html>)



- Phloroglicinol: HO

Figure 17: Structure of Phloroglicinol (<http://www.wikiwand.com/nl/Floroglucinol>)

1.6.4.5 Lignin

Lignin is a complex organic compound that binds to cellulose fibers and hardens and strengthens the cell walls of plants. Lignin is a polymer consisting of various aromatic alcohols and is the chief non-carbohydrate constituent of wood. The composition of lignin varies from species to species.

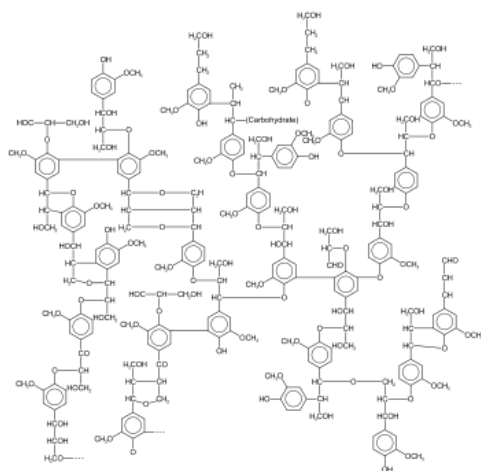


Figure 18: Chemical structure of lignin (<https://en.wikipedia.org/wiki/Lignin>)

1.7 FAAS

1.7.1 Instrumental set-up

Flame Atomic Absorption Spectrometry is a method used for the quantitative determination of chemical elements by using the absorption of optical radiation by free atoms in the gaseous state.

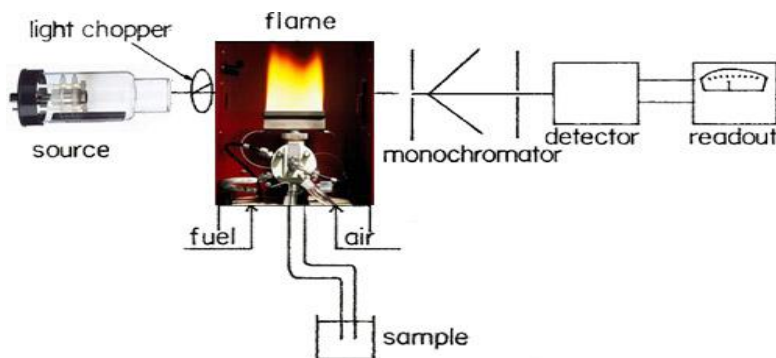


Figure 19: Sketch of the components of the FAAS

(http://faculty.sdmiramar.edu/fgarces/labmatters/instruments/aa/AAS_Theory/AASTheory.htm)

1.7.2 Instrument components

1.7.2.1 Hollow cathode lamp

The light source in the AAS is called a hollow cathode lamp. The light from this lamp is the light required for the analysis. There is no need for a monochromator because the atoms of the metal that are tested are present within the lamp. When the lamp is on, these atoms are supplied with energy, which causes them to elevate to the excited states. Upon returning to the ground state, exactly the same wavelengths that are useful in the analysis are emitted.

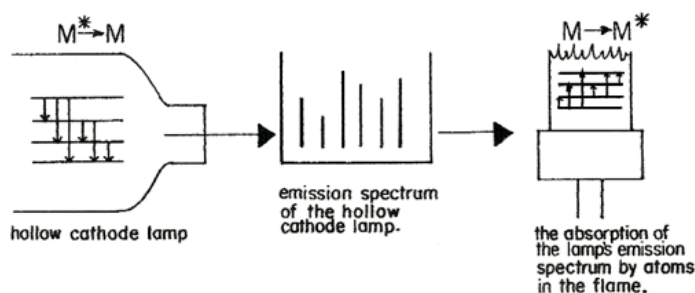


Figure 20: Illustration of the method of the hollow cathode lamp

(http://faculty.sdmiramar.edu/fgarces/labmatters/instruments/aa/AAS_Theory/AASTheory.htm)

Therefore, the hollow cathode lamp must contain the element being determined. Some lamps are multi element, which means that several different kinds of atoms are present in the lamp.

1.7.2.2 Burners

The fuel and oxidant are forced,, under pressure, into the flame, whereas the sample is drawn into the flame by aspiration.

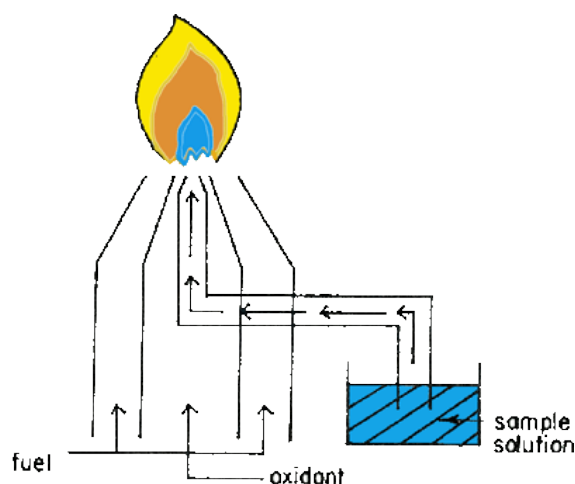


Figure 21: The nebulizer

(http://faculty.sdmiramar.edu/fgarces/labmatters/instruments/aa/AAS_Theory/AASTheory.htm)

But the resulting flame is turbulent and non-homogenous, a property that negates its usefulness in AA, since the flame must be homogenous. The premix burner however does away with this difficulty.

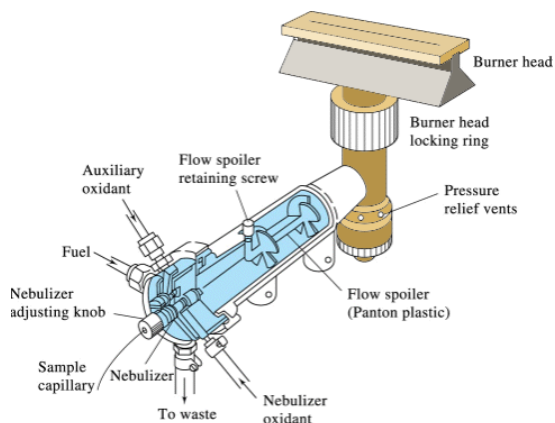


Figure 22: The premix burner

(http://faculty.sdmiramar.edu/fgarces/labmatters/instruments/aa/AAS_Theory/AASTheory.htm)

The fuel, oxidant and sample all meet at the base of the flame and is premixed before entering the flame.

1.7.2.3 Flame

All flames require both a fuel and an oxidant in order to exist. In this bachelor thesis the FAAS was equipped with a flame that used oxygen as an oxidant and acetylene as a fuel. A maximum temperature of 2300 K can be achieved in such a flame. The temperature could be raised when pure oxygen is used but such a flame suffers from the disadvantage of a high burning velocity, which decreases the completeness of the atomization and therefore lowers the sensitivity.

In the flame, there is a process that consist of different stages:

1. Desolvation: the process of evaporation of the solvent from an aerosol of fine droplets and the dry sample particles remain.
2. Vaporization: particles converted into gaseous molecules.
3. Atomization: the conversion of volatilized analyte into free atoms.
4. Ionization: atoms can be partial converted into gaseous ions.

1.7.2.4 Monochromator

A monochromator is used to select the specific wavelength of light, which is absorbed by the sample. The light selected by the monochromator is directed onto a detector. The detector is typically a photomultiplier tube. This tube produces an electrical signal proportional to the light intensity.

1.7.2.5 Readout component

The readout of the absorbance and transmittance data consist of a digital readout. The concentration is automatically presented by the computer after the data is transmitted by the reader.

2 OBJECTIVES

The general purpose of this research is to separate metals from the binary mixtures solutions Ni-Cu and Cd-Pb by using grape stalks in fixed columns. To achieve this objective, flow up columns filled with grape stalks will be used. The effect of two parameters will be studied.

- 1) The effect of bed lengths on metal separation of two binary metal mixtures will be studied. To do this, fixed column filled with 2, 1 and 0,5 g of grape stalks will be used.
- 2) Secondly, the effect of metal concentrations on metal separation will be studied. Different ratio's between Ni-Cu and Cd-Pb concentrations will be used by using the same bed length.
- 3) Experimental results will be modelled by using the Bed Depth Service Time Model to predict the separation time of Cu-Ni and Cd-Pb from binary metal mixtures, at different conditions.

3 **EXPERIMENTAL PART**

3.1 MATERIALS AND METHODS

3.1.1 Grape stalks

3.1.1.1 Occurrence

The grape stalk used in this bachelor thesis were kindly supplied by a wine manufacturer of the Empordà- Costa Brava region, Girona, Spain.



Figure 23: Vineyard in the Costa Brava (northern Spain)

3.1.1.2 Grape stalks preparation

The branches of the grape stalks can't be used to fill up the fixed beds. First the usable parts of the grape stalks were cut into small pieces with a scissor. Then the small pieces were washed with distilled water and with milli-Q water, dried in an oven by 55 degree Celsius. Finally the dried pieces were sieved for a particle size of 0,25-0,50 mm. The particle size of the grape stalks that can be used for the most efficient uptake of metals has been studied in previous work. (Oñate, 2009).



Figure 24: Grinder (Pro prop cuisine art)



Figure 25: Parts of interest of grape stalks



Figure 26: Automatic siever (CISA)



Figure 27: Sieved grape stalks with a particle size between 250 and 500 μm

3.1.1.3 Preparation of the column

The fixed bed sorption experiments were carried out in glass columns of 10 cm length and 1,0 cm inner diameter. The column was washed with milli-Q water. The column was then packed with grape stalks and if needed glass pearls to fill up the bed. Glass wool was used as a filter.



Figure 28: Glass wool



Figure 29: Fixed bed filled with grape stalks

3.1.2 Experimental set-up

Figure 30 represents the experimental set-up.

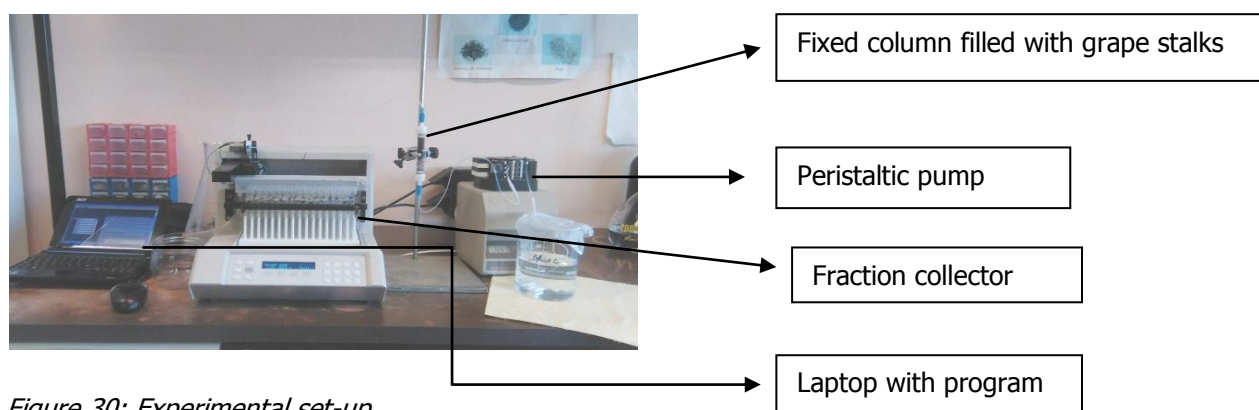


Figure 30: Experimental set-up

The experimental set-up consists out of a peristaltic pump, a fixed bed, a fraction collector and a laptop to coordinate the fraction collector. the tubes that are used to connect the fraction collector with the column and to connect the column with the pump have a colour code that represent the characteristics of the tubes. The tubes used for the experiments had a colour code gray-gray. More information about the different colour codes of the tubes can be found in the annex.

3.1.3 Flow rate

The flow rate was set at 30 ml/hour for every experiment performed. Good results were obtained by using this flow rate in previous works regarding the metal uptake by grape stalks for the binary metal mixtures of Cu/Ni and Cd/Pb. (Oñate, 2009)

3.1.4 Analysis of the metals

3.1.4.1 FAAS

The analysis of the metal uptake by grape stalks was performed with the flame atomic absorber spectrometer.

3.1.4.2 Lamps

For the analyses of copper and nickel a multi element was used. This means that both metals could be analysed by using only one lamp. To analyse cadmium and lead different lamps were used. The lamp was positioned in position 1 for all experiments regarding the study of the bed length. For the study of the concentration range the lamp position was 2.

3.1.4.3 Automatic dilutor

An automatic diluter SIPS of the mark Varian was used to analyse higher metal concentrations. The automatic dilutor was connected with the FAAS and could be used directly during the analyses.

3.1.5 Stock solutions

3.1.5.1 Copper

Copper standards were prepared from a copper standard solution of 1000 mg/L. The copper standards had to be prepared in a range from 0,1-10 mg/L because the calibration curve with the FAAS of copper goes from 0,1-10 mg/L. Copper standards of 10 mg/L Cu, 8 mg/L Cu, 5 mg/L Cu, 2 mg/L Cu and 1 mg/L Cu were prepared.

Working conditions for copper on the FAAS:

The wavelength used during the analyses on the FAAS for copper was 324,7 nm. The optimum working range lays between 0 and 10 mg/L. The lamp current was 4 mA. Acetylene was used as fuel with a support of air.

3.1.5.2 Nickel

Nickel standards were prepared from a nickel standard solution of 1000 mg/L. The nickel standards had to be prepared in a range from 0,1-20 mg/L because the calibration curve with the FAAS of nickel goes from 0,1-20 mg/L. Nickel standards of 20 mg/L Ni, 15 mg/L Ni, 10 mg/L Ni, 5 mg/L Ni and 1 mg/L Ni were prepared. The initial concentration of the nickel solutions made for the experiments were higher than the concentrations of the calibration curve. For this reason the automatic diluter was used to dilute the high concentrations of nickel while measuring. The automatic diluter had to be calibrated before use. From a standard of 20 mg/L three other standards were automatically measured with the automatic diluter.

Working conditions for nickel on the FAAS:

The wavelength used during the analyses on the FAAS for nickel was 232,0 nm. The optimum working range lays between 0,1 and 20 mg/L. The lamp current was 4 mA. Acetylene was used as fuel with a support of air.

3.1.5.3 Lead

Lead standards were prepared from a lead standard solution of 1000 mg/L. The lead standards had to be prepared in a range from 0,1-30 mg/L because the calibration curve with the FAAS of lead goes from 0,1-30 mg/L. Lead standards of 25 mg/L Cu, 20 mg/L Cu, 15 mg/L Cu, 10 mg/L Cu and 5 mg/L Cu were prepared.

Working conditions for lead on the FAAS:

The wavelength used during the analyses on the FAAS for lead was 405,8 nm. The optimum working range lays between 0,1 and 30 mg/L. The lamp current was 4 mA. Acetylene was used as fuel with a support of air.

3.1.5.4 Cadmium

Cadmium standards were prepared from a cadmium standard solution of 1000 mg/L. The cadmium standards had to be prepared in a range from 0,02-3 mg/L because the calibration curve with the FAAS of lead goes from 0,02-3 mg/L. Cadmium standards of 3 mg/L Cu, 2,5 mg/L Cu, 2 mg/L Cu, 1 mg/L Cu and 0,5 mg/L Cu were prepared.




Working conditions for cadmium on the FAAS:

The wavelength used during the analyses on the FAAS for cadmium was 326,1 nm. The optimum working range lays between 0,02 and 3 mg/L. The lamp current was 4 mA. Acetylene was used as fuel with a support of air.

3.1.6 preparation of the columns

The first parameter that was studied was the bed length. Three fixed beds were filled with each a different amount of grape stalks. The concentration of the metals in the binary metal mixtures remain unchanged during these experiments. The sequence of the experiments is the same as in the table shown below.

Table 3: Summary of the study of the bed length

Bed length of grape stalks	Amount of grape stalks	Photo of the column
Full bed = 7 cm	2,0 g	
Half filled bed = 3,5 cm	1,0 g	
Quarter filled bed = 1,75 cm	0,5 g	

3.1.7 Metal mixtures

3.1.7.1 Heavy metal solutions

The heavy metal solutions were made in flat bottomed flasks of 2 L. Every solution consisted of two different metals. Two different binary metal mixtures were made for each parameter that was studied. A metal mixture of copper and nickel and a metal mixture of cadmium and lead. The uptake of binary metal mixtures of Cu/Ni and Cd/Pb have been studied in previous work. These metal mixtures gave good results for sorption uptake by grape stalks (Oñate, 2009). The metal concentrations were changed to study the difference in metal separation with different metal concentrations in binary metal mixtures. The first parameter that was studied was the bed length. The bed length was changed but the concentrations of the binary metal mixtures were fixed.

The second parameter that was studied was the concentration ratio between the two metals present in the binary metal mixture. In this case the bed length was fixed.

In the table below the concentration of the metals used in the binary metal mixtures are presented.

Table 4: Concentration of the metals used in the binary metal mixtures

Metal mixture of Ni/Cu	Ni (mg/L)	Cu (mg/L)	Metal mixture of Cd/Pb	Cd (mg/L)	Pb (mg/L)
1	145	5,4	6	52	45
2	145	14,5	8	52	20
3	145	35	9	52	9
4	145	72	10	52	3
5	145	145			

The metal mixtures used in this work are presented in the table above. The metal concentrations of the metal mixtures 1 and 6 were selected to simulate the actual concentrations of the heavy metals in the river Odiel in Northern Spain. To make the binary solutions following products were used:

- Copper(II) chloride dehydrate
- Nickel(II) chloride hexahydrate
- Lead(II) chloride
- Cadmium(II) chloride 2,5 hydrate

3.1.7.2 Calculations of metal mixture 1 of Cu and Ni

5,4 mg/L Cu and 145 mg/L Ni was needed to make the binary metal mixtures for the different bed lengths.

Calculations

$$\text{Mr}(\text{CuCl}_2 \cdot 2\text{H}_2\text{O}) = 170,48$$

$$\text{Mr}(\text{Cu}) = 63,55$$

$$\text{Mr}(\text{NiCl}_2 \cdot 6\text{H}_2\text{O}) = 237,69$$

$$\text{Mr}(\text{Ni}) = 58,69$$

- $5,4 \text{ mg/L Cu} * 2 = 10,8 \text{ mg/L Cu}$
 $63,55 \text{ g/mol Cu} \rightarrow 0,0108 \text{ g Cu}$
 $170,48 \text{ g/mol CuCl}_2 \cdot 2\text{H}_2\text{O} \rightarrow 0,0289 \text{ g CuCl}_2 \cdot 2\text{H}_2\text{O}$
 $0,028 \text{ g CuCl}_2 \cdot 2\text{H}_2\text{O}$ was weighed on the balance.
 The weighed product was then dissolved in a volumetric flask of 2 L with milli Q water.
- $145 \text{ mg/L Ni} * 2 = 290 \text{ mg/L Ni}$
 $58,69 \text{ g/mol Ni} \rightarrow 0,290 \text{ g Ni}$
 $237,69 \text{ g/mol NiCl}_2 \cdot 6\text{H}_2\text{O} \rightarrow 1,174 \text{ g NiCl}_2 \cdot 6\text{H}_2\text{O}$
 $1,172 \text{ g NiCl}_2 \cdot 6\text{H}_2\text{O}$ was weighed on the balance.
 The weighed product was then dissolved in a volumetric flask of 2 L with milli Q water.

The other metal mixtures of Copper and nickel were calculated the same way as the calculation that were made for metal mixture 1.

3.1.7.3 Calculations of metal mixture 6 of Pb and Cd

45 mg/L Pb and 52 mg/L Ni was needed to make the binary metal mixtures for the different bed lengths.

Calculations

$$M (\text{CdCl}_2 \cdot 2,5 \text{ H}_2\text{O}) = 228,3544 \text{ g/mol}$$

$$M (\text{Cd}) = 112,411 \text{ g/mol}$$

$$M (\text{PbCl}_2) = 278,105 \text{ g/mol}$$

$$M (\text{Pb}) = 207,2 \text{ g/mol}$$

- $52 \text{ mg/L Cd} * 2 = 104 \text{ mg/L Cd}$
 $112,411 \text{ g/mol Cd} \rightarrow 0,104 \text{ g Cd}$
 $228,3544 \text{ g/mol CdCl}_2 \cdot 2,5 \text{ H}_2\text{O} \rightarrow 0,211 \text{ g CdCl}_2 \cdot 2,5 \text{ H}_2\text{O}$
 $0,213 \text{ g CdCl}_2 \cdot 2,5 \text{ H}_2\text{O}$ was weighed on the balance.
 The weighed product was then dissolved in a volumetric flask of 2 L with milli Q water.
- $45 \text{ mg/L Pb} * 2 = 90 \text{ mg/L Pb}$
 $207,2 \text{ g/mol Pb} \rightarrow 0,090 \text{ g Pb}$
 $278,105 \text{ g/mol PbCl}_2 \rightarrow 0,1208 \text{ g PbCl}_2$
 $0,122 \text{ g PbCl}_2$ was weighed on the balance.
 The weighed product was then dissolved in a volumetric flask of 2 L with milli Q water.

The other metal mixtures of Cadmium and Lead were calculated the same way as the calculation that were made for metal mixture 6 above.

4 RESULTS

4.1 EFFECT OF THE BED LENGTH

4.1.1 Experiments of Copper and nickel with different bed length

4.1.1.1 Binary mixture of Cu/Ni with a full column (2 g of grape stalks)

In figure 31 the breakthrough curve of copper with a full column is presented. Copper and nickel are presented individually because the initial concentration of both metals lies far apart.

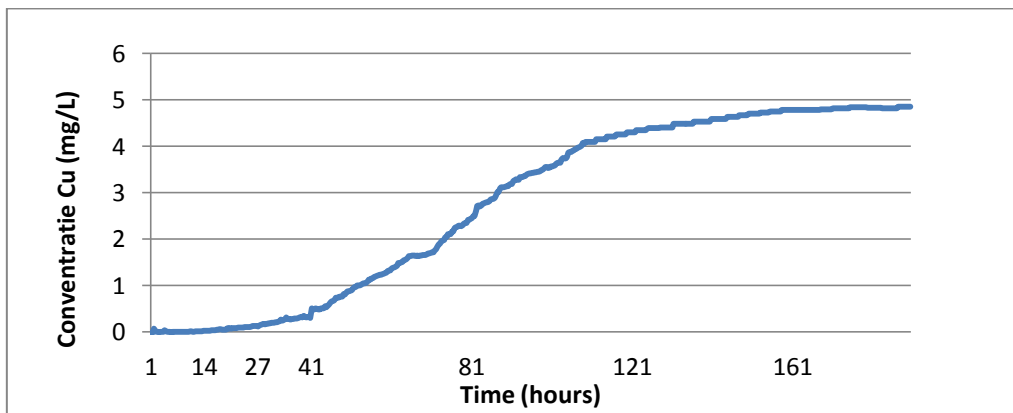


Figure 31: Breakthrough curve of copper with a full column (conditions: $C_{i, cu} = 5,78 \text{ mg/L}$; $C_{i, ni} = 155 \text{ mg/L}$; column length = 7 cm)

As observed in the figure above, the S-curve that is typical for a good breakthrough curve is visible. The concentration of copper is zero in the beginning and starts to increase after several hours. This means that 100 % copper is sorbed by the grape stalks in those hours. After 15 hours, copper is not completely sorbed as could be concluded by analysing the results.

In figure 32 the breakthrough curve of nickel with a full column is presented.

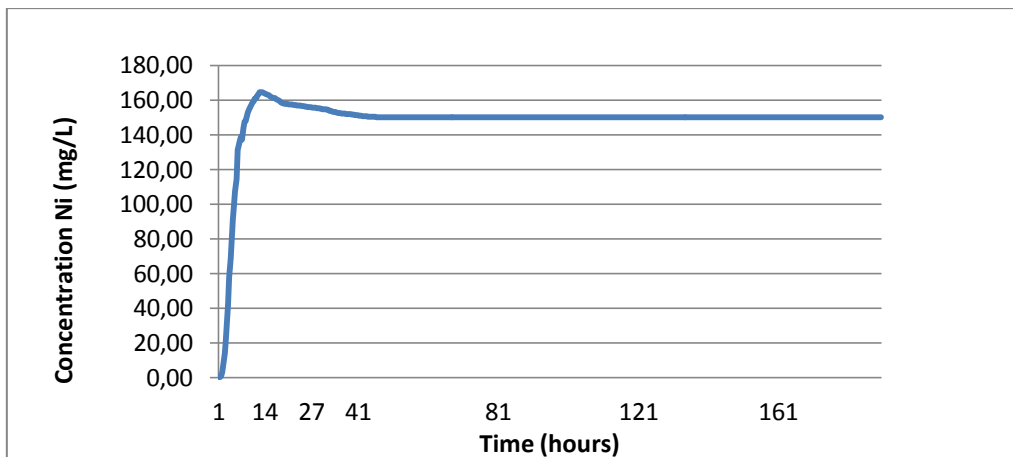


Figure 32: Breakthrough curve of nickel with a full column (conditions: $C_{i, cu} = 5,78 \text{ mg/L}$; $C_{i, ni} = 155 \text{ mg/L}$; column length = 7 cm)

As observed in figure 32, there is no S-shape visible. The nickel concentration starts to increase almost directly. After a few hours the initial concentration of nickel gets surpassed as can be seen in figure 33 where the nickel concentration shows a hump. This hump is called an overshoot. When the overshoot is reached, part of the metal, in this case nickel, is released or desorbed from the column. The concentration of nickel by the outflow of the column, when the overshoot happens, is more than the initial concentration of nickel. Figure 33 represents the breakthrough curve of the binary metal mixture of copper and nickel with a full column.

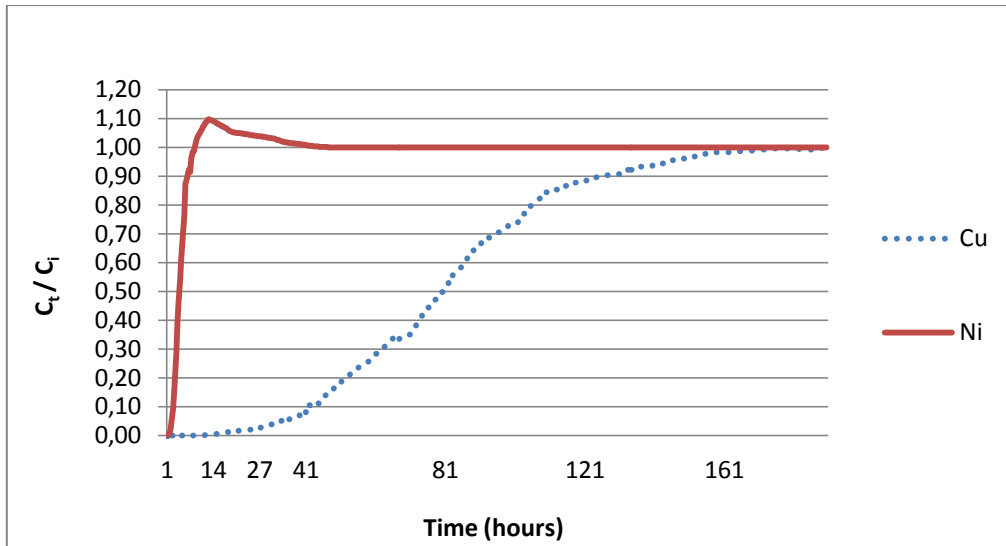


Figure 33: Breakthrough curve of copper and nickel with a full column (conditions: $C_{i, cu} = 5,78 \text{ mg/L}$; $C_{i, ni} = 155 \text{ mg/L}$; column length = 7 cm; flow rate = 30 ml/hour, C_f/C_i = concentration of the metal divided by the initial concentration)

In the figure above the y-axis presents the ratio between the concentration and the initial concentration of each metal. The first hour no metal is detected so both copper and nickel are sorbed during this hour. After one hour, the solution contains nickel. From the second hour until after 15 hours, only nickel is detected. This means that copper is sorbed by grape stalk and nickel is not sorbed in those 14 hours. The hours when copper is sorbed and nickel not is called the separation time. The separation volume can be obtained from the flow rate given in the caption of figure 33. The volume passed during the 14 hours of separation is 1,07 L. As can be seen there is a good nickel separation during this time. After 9 hours the overshoot of nickel is visible.

This overshoot is probably due to the exchange between Copper and nickel sorption onto the grape stalks. Copper does not overshoot because it has a greater affinity than nickel does for grape stalks.

4.1.1.2 Binary mixture of Cu/Ni with a half filled column (1 g of grape stalks)

In figure 34 the breakthrough curve of copper with a half-filled column is presented. Copper and nickel are presented individually because the initial concentration of both metals lies far apart.

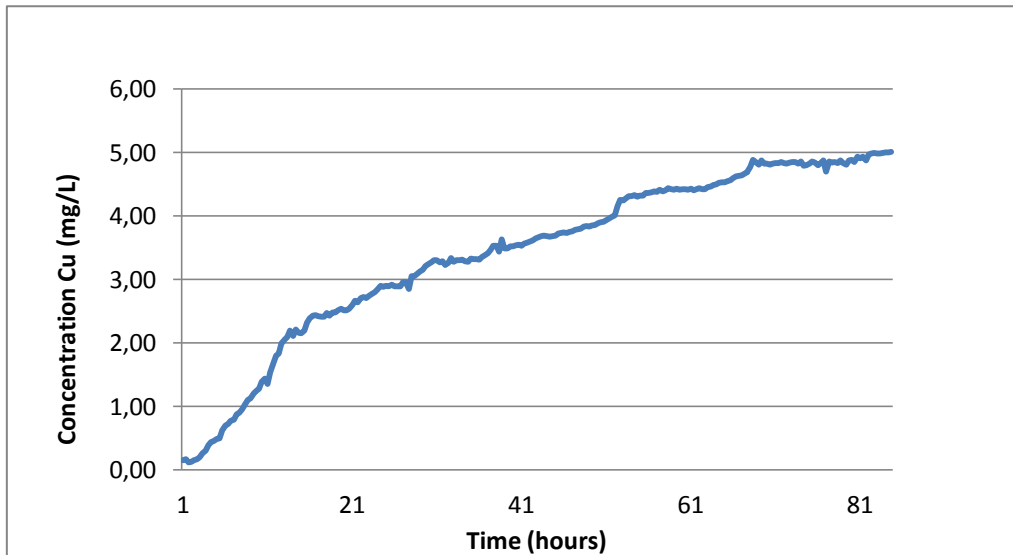


Figure 34: Breakthrough curve of copper with a half filled column (conditions: $C_{i, cu} = 5,25 \text{ mg/L}$; $C_{i, ni} = 131,04 \text{ mg/L}$; column length = 3,5 cm)

In the figure above the S-shape is not clearly visible. Not all copper is sorbed in the first hours as can be seen in the figure above. The concentration of copper increases continuously in a linear tendency

In figure 35 the breakthrough curve of nickel with a half-filled column is presented.

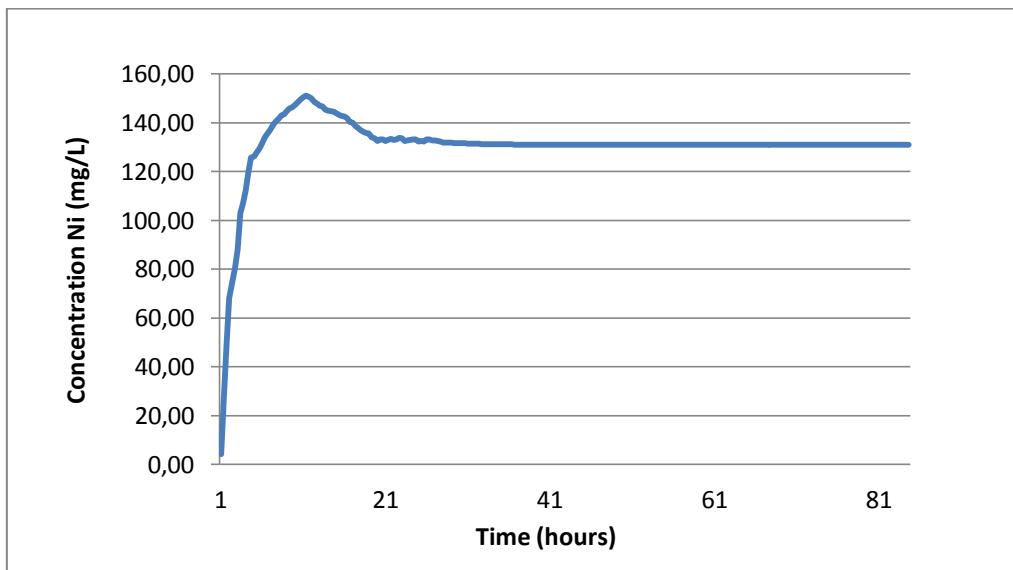


Figure 35: Breakthrough curve of nickel with a half filled column (conditions: $C_{i, cu} = 5,25 \text{ mg/L}$; $C_{i, ni} = 131,04 \text{ mg/L}$; column length = 3,5 cm)

Nickel is never totally sorbed and thus the concentration of nickel increases rapidly until the overshoot is reached.

Figure 36 represents the breakthrough curve of the binary metal mixture of copper and nickel with a half-filled column.

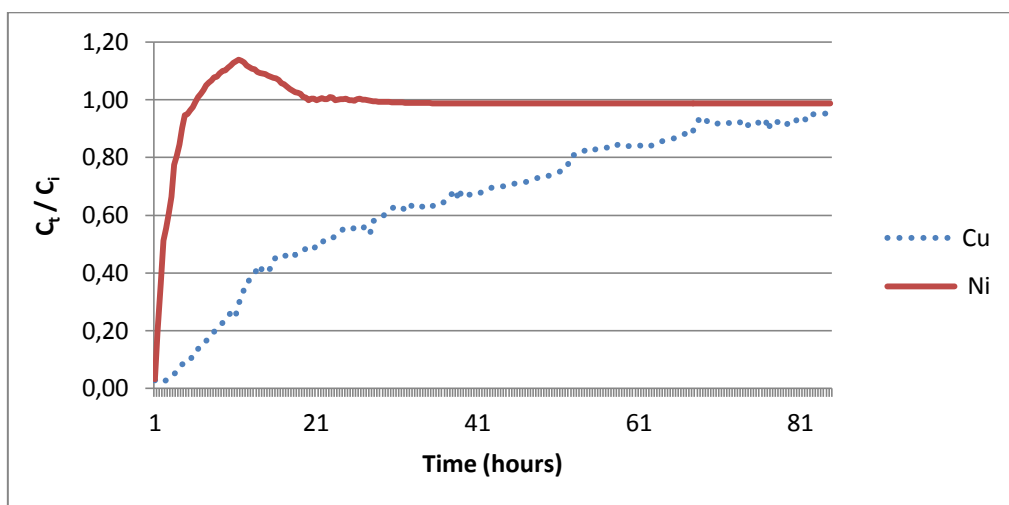


Figure 36: Breakthrough curve of copper and nickel with a half filled column (conditions: $C_{i, cu} = 5,25$ mg/L; $C_{i, ni} = 131,04$ mg/L; column length = 3,5 cm; flow rate = 30 ml/hour)

During the first four hours only copper is totally sorbed by the grape stalks. Thus the first four hours there is separation between copper and nickel. 0,1 L of nickel solution is separated by using the experimental conditions. An overshoot of nickel is clearly visible in figures 36 and 37. The initial concentration of copper is not reached after more than 81 hours as can be seen in the figure above. The results indicate that the experimental conditions used are not effective to obtain a big volume of nickel solution.

4.1.1.3 Binary mixture of Cu/Ni with a quarter filled column (0,5 g of grape stalks)

In figure 37 the breakthrough curve of copper with a quarter-filled column is presented. Copper and nickel are presented individually because the initial concentration of both metals lie far apart.

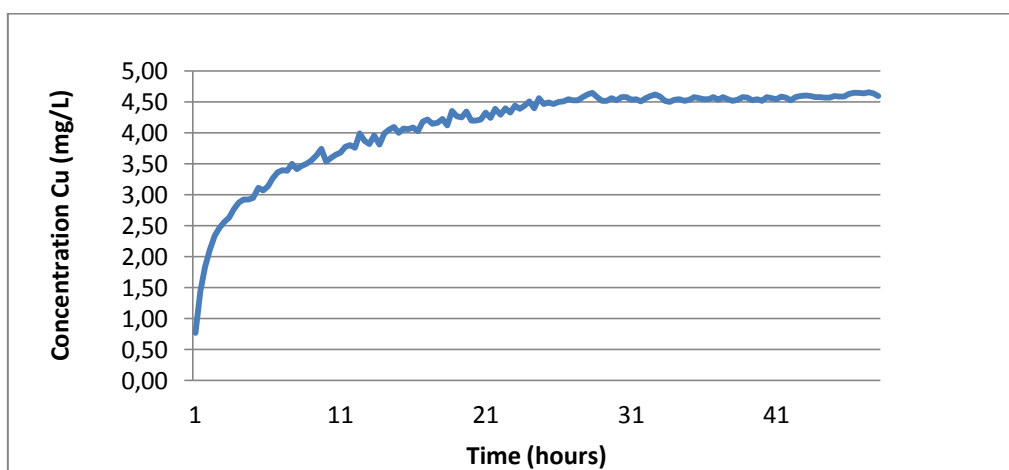


Figure 37: Breakthrough curve of copper with a column filled with 0,5 g of grape stalks (conditions: $C_{i, cu} = 4,95$ mg/L; $C_{i, ni} = 160,0$ mg/L; column length = 1,75 cm)

There is no S-shape visible in figure 37. Copper is never totally sorbed.

In figure 38 the breakthrough curve of nickel with a quarter-filled column is presented.

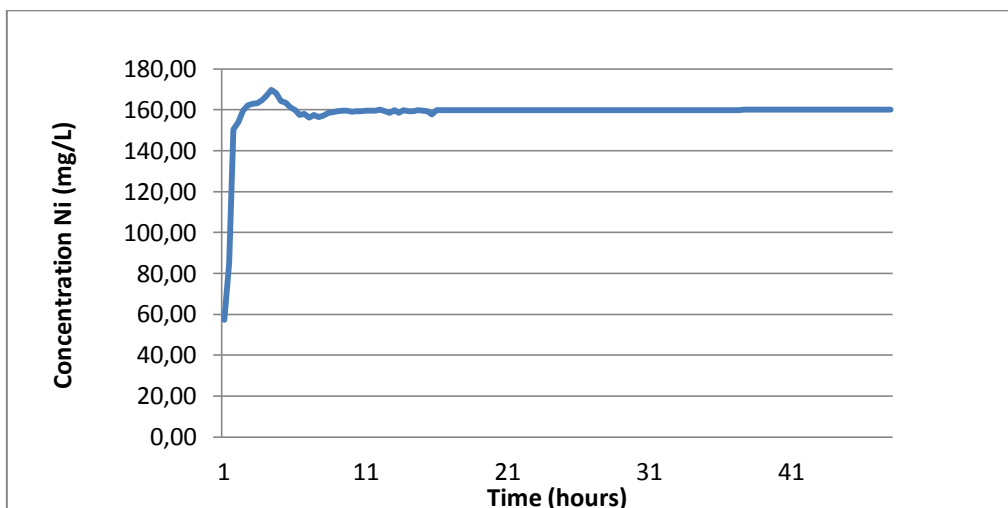


Figure 38: Breakthrough curve of nickel with a column filled with 0,5 g of grape stalks (conditions: $C_{i, cu} = 4,95$ mg/L; $C_{i, ni} = 160,0$ mg/L; column length = 1,75 cm)

The nickel concentration increases rapidly in the first three hours. Nickel concentration is never totally sorbed.

Figure 39 represents the breakthrough curve of the binary metal mixture of copper and nickel with a quarter-filled column.

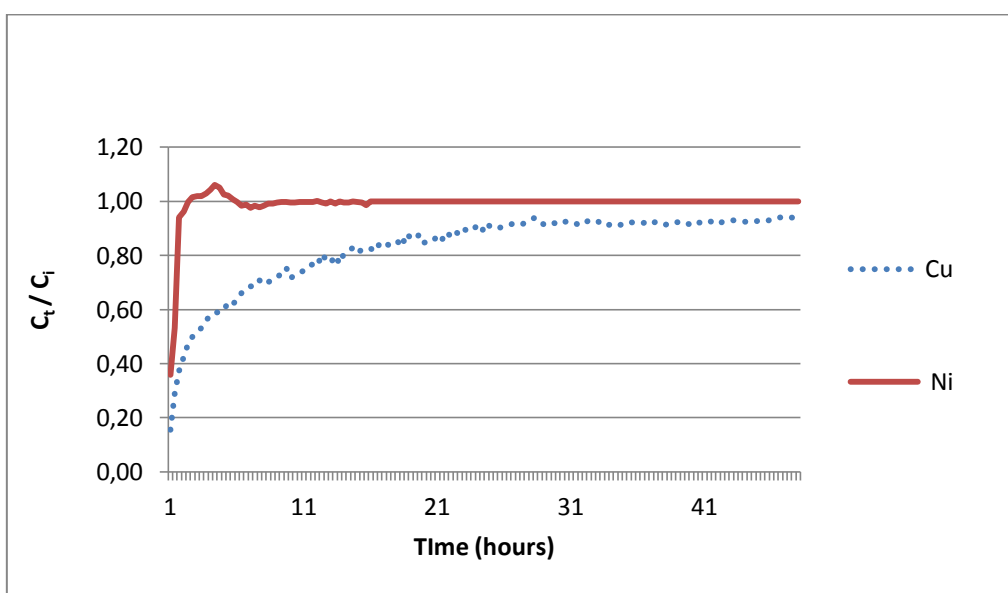


Figure 39: Breakthrough curve of copper and nickel with a column filled with 0,5 g of grape stalks (conditions: $C_{i, cu} = 4,95$ mg/L; $C_{i, ni} = 160,0$ mg/L; column length = 1,75 cm; flow rate = 30 ml/hour)

There is no separation between the two metals. Both copper as nickel are not totally sorbed. The initial concentration of copper is not reached after 50 hours as can be seen by the little gap between the lines of copper and nickel at the end of the plot in the figure above.

4.1.1.4 Summary of the study of the bed length with copper and nickel

In the table below the summary of the study of the bed length as a function of the initial concentration of copper and nickel is presented. The value Q, the amount of metal sorbed in mg per g of grape stalks is also presented.

Table 5: Summary of the study of the bed length with copper and nickel

Bed length	Separation time (hours)	Cu		Ni	
		Initial concentration Cu (mg/L)	Q (mg/g)	Initial concentration Ni (mg/L)	Q (mg/g)
7 cm	14	4,86	5,92	150,00	5,91
3,5 cm	1	5,25	4,66	132,66	5,73
1,75 cm	0	4,95	2,45	160,00	5,79

As can be seen in table 5, the separation of the binary metal mixture in the conditions used in the previous experiments, is not possible when the bed length of 1,75 cm is used. the Q values for copper are not similar. The Q value of copper with a bed length of 1,75 cm is lower than the full of half-full column. This could be due to the short contact time between the metal ions and the grape stalks. Also, the experiment with the shortest bed length wasn't finished, the initial concentration of copper wasn't reached. Conversely, the Q values of nickel sorbed are close to each other indicating that the material was saturated.

4.1.2 Experiments with Cadmium and lead with different bed length

4.1.2.1 Binary mixture of Cd/Pb with a full column (2 g of grape stalks)

In figure 40 the breakthrough curve of lead and cadmium is presented as a function of time with a full column. The initial concentration of lead and cadmium are close to each other so the figures that will follow contain both metals instead of presenting the breakthrough curves of the metals separately.

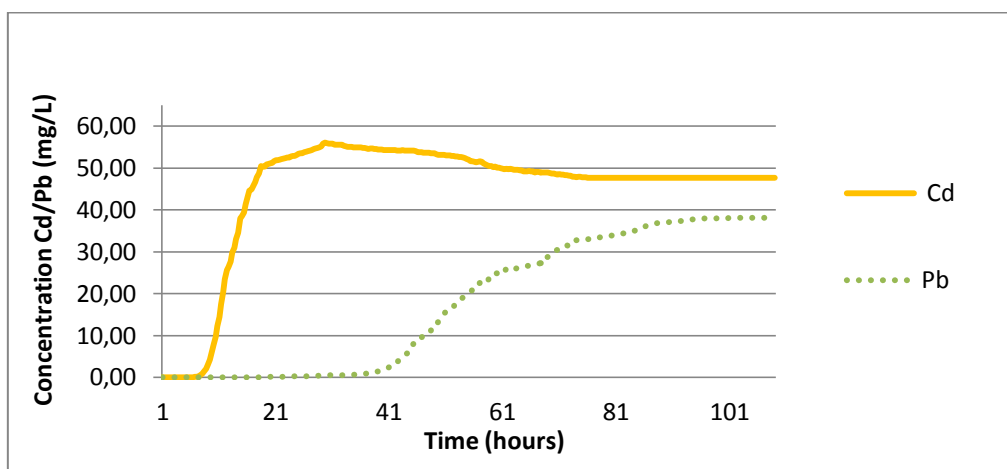


Figure 40: Breakthrough curve of lead and cadmium with a full column (conditions: $C_{i, Pb} = 40,38$ mg/L; $C_{i, Cd} = 47,67$ mg/L; column length = 7 cm; flow rate = 30 ml/hour)

During the first hours both lead and cadmium are sorbed by the grape stalks. After a few hours, the cadmium concentration starts to increase. After 20 hours cadmium overshoots. The overshoot is long as can be seen in figure 40. Lead is sorbed for a long time and the concentration starts to increase when the overshoot of cadmium is almost ended. The S-curve of lead and cadmium is visible.

Figure 41 presents the breakthrough curve of cadmium and lead with in the y-axis C_t / C_i and in the x-axis the time.

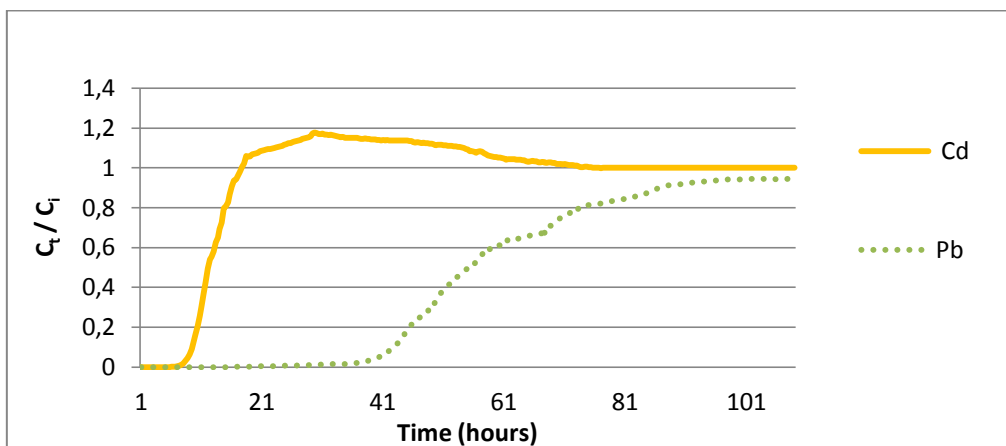


Figure 41: Breakthrough curve of lead and cadmium with a full column (conditions: $C_{i, Pb} = 40,38$ mg/L; $C_{i, Cd} = 47,67$ mg/L; column length = 7 cm; flow rate = 30 ml/hour)

The first six hours no metal is measured in the outflow solution, thus both metals are totally sorbed by the grape stalks. After six hours the cadmium concentration increases rapidly until the overshoot is reached. A big and long overshoot of cadmium appears after 18 hours and ends after 52 hours. Lead concentration starts to increase after 16 hours. Cadmium is separated from lead for 10 hours or for 0,42 litres of initial metal mixture solution.

4.1.2.2 Binary mixture of Cd/Pb with a half filled column (1 g of grape stalks)

In figure 42 the breakthrough curve of lead and cadmium with a half filled column is presented.

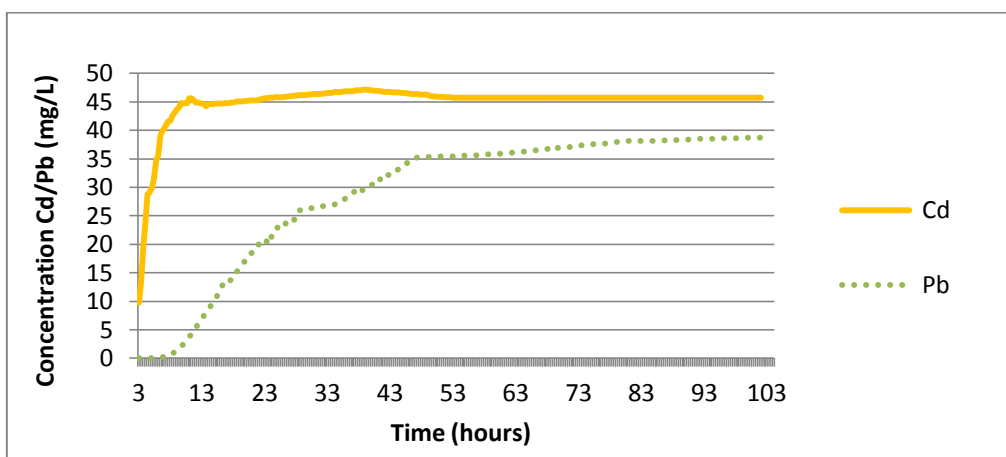


Figure 42: Breakthrough curve of Pb and Cd with a half filled column (conditions: $C_{i, Pb} = 40,93$ mg/L; $C_{i, Cd} = 45,71$ mg/L; column length = 3,5 cm; flow rate = 30 ml/hour)

From the start lead is totally sorbed and cadmium only partially sorbed. Cadmium concentration increases immediately during the first hours. The breakthrough curve of lead presents a S-shape.

Figure 43 presents the breakthrough curve of cadmium and lead with in the y-axis C_t/C_i and in the x-axis the time.

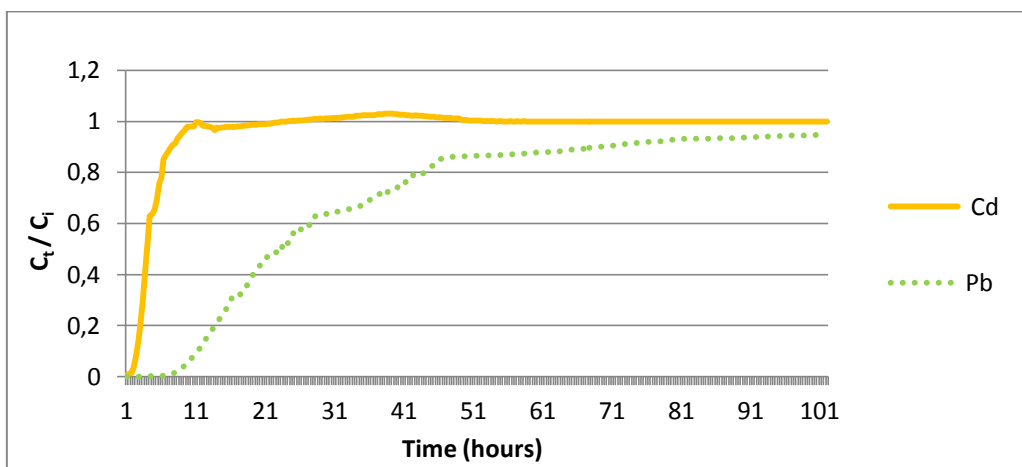


Figure 43: Breakthrough curve of Pb and Cd with a half filled column (conditions: $C_{i, Pb} = 40,93 \text{ mg/L}$; $C_{i, Cd} = 45,71 \text{ mg/L}$; column length = 3,5 cm; flow rate = 30 ml/hour)

Again there is a separation between both metals. Cadmium ions are separated from lead in the binary mixture for 6 hours. About 0,16 litres of solution goes through the column when separation takes place. In this case, there is no overshoot of cadmium observed.

4.1.2.3 Binary mixture of Cd/Pb with a quarter filled column (0,5 g of grape stalks)

In figure 44 the breakthrough curve of lead and cadmium with a quarter filled column is presented.

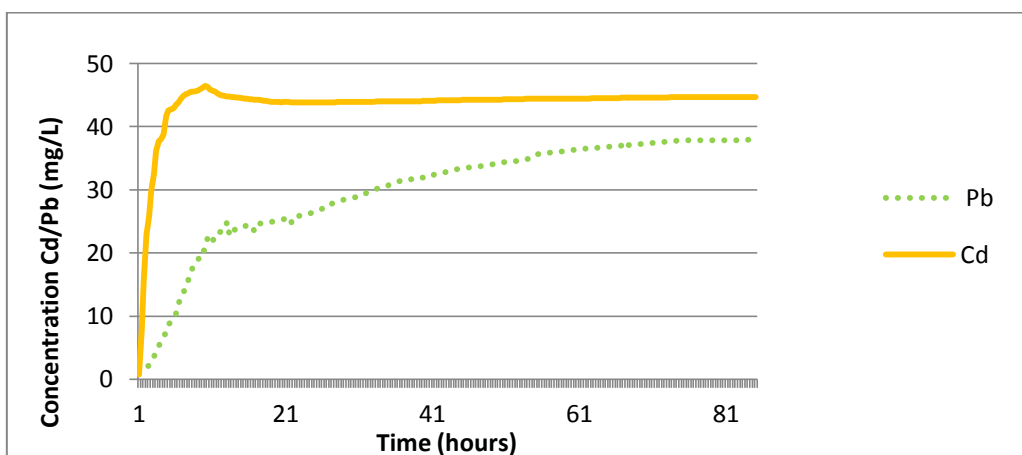


Figure 44: Breakthrough curve of Pb and Cd with a column filled with 0,5 g of grape stalks

Both metal concentrations increase rapidly during the first hours. Nor cadmium nor lead are totally sorbed. There is a little overshoot of cadmium visible for 4 hours. The plot of lead doesn't resemble a S-shape.

Figure 45 presents the breakthrough curve of cadmium and lead with in the y-axis C_t / C_i and in the x-axis the time.

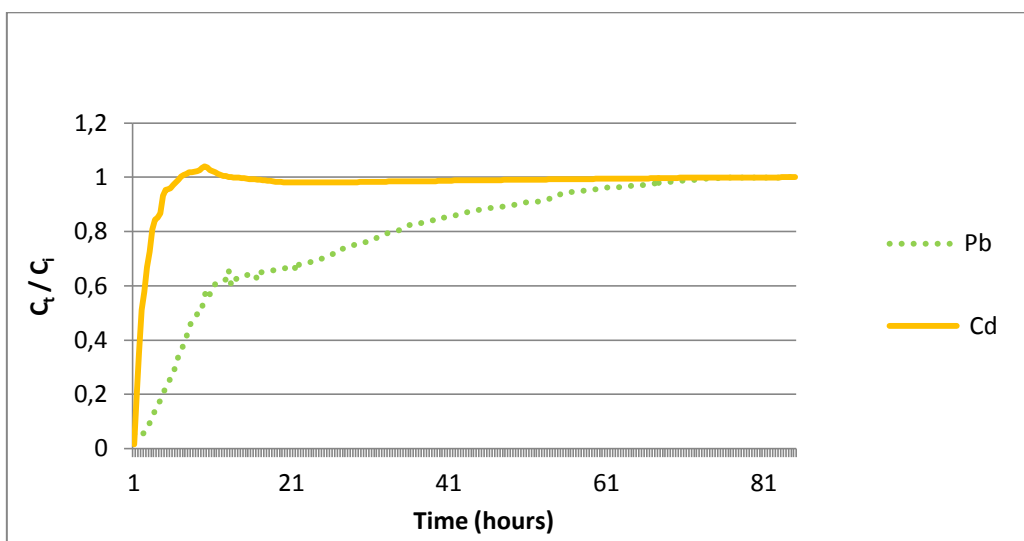


Figure 45: Breakthrough curve of Pb and Cd with a column filled with 0,5 g of grape stalks

As can be seen in figure 45, metals cannot be separated in these experimental conditions. There is no separation of cadmium and lead ions probably due to the short bed length used.

4.1.2.4 Summary of the study of the bed length with lead and cadmium

In the table below the study of the bed length for the binary metal mixture of cadmium and lead is summarized.

Table 6: Summary of the parameter bed length

Bed length	Separation time (hours)	Cd		Pb	
		Initial concentration Cd (mg/L)	Q (mg/g)	Initial concentration Pb (mg/L)	Q (mg/g)
7 cm	6	47,67	4,53	40,38	35,94
3,5 cm	0	45,71	4,73	40,93	37,81
1,75 cm	0	37,89	4,58	44,70	39,92

The Q values by each metal should be the same for the different bed lengths when the grape stalk is saturated. This is the case for lead and almost the case for cadmium. The high values of Q for lead can be attributed to different aspects. The first aspect is the higher molar mass of lead (207,2 g/mol) in comparison with cadmium (112,4 g/mol). The second aspect is the difference in the number of active sites linked for lead. There was separation only when the full bed length was used.

From these experimental results we conclude that when the bed length is highest (7 cm), the volume of metal separated is higher. All next experiments will be performed with full bed length (7 cm filled with grape stalks).

4.2 EFFECT OF METAL CONCENTRATIONS

After the bed length was defined, the concentration ratio for metal separation was studied. The concentrations of copper and lead were changed to obtain different concentration ratio's in the binary metal mixtures. The purpose of this study is to find out if there is separation between the binary metal mixtures when the concentration ratio's were changed. Therefore, the experiments don't have to be finished until the initial concentration is reached. Only the beginning of the experiments are of interest. The relationship between the concentration and the separation volume until the breakthrough point is reached is studied. The breakthrough point occurs when the concentration of the fluid leaving the bed spikes as unabsorbed solute begins to emerge. At this point, the bed becomes ineffective for the separation of metals in mixtures. In this work the breakthrough point is selected at 1 mg/L. In table 7 the concentration ratio's of the binary metal mixtures experimented are presented.

Table 7: Concentrations ratio's used in the binary metal mixtures

Concentration ratio's Cu/Ni	Concentration Cu (mg)	Concentration Ni (mg)	Concentration ratio's Pb/Cd	Concentration Pb (mg)	Concentration Cd (mg)
1/27	5,4	145	1/15	3	40
1/10	14,5	145	1/5	9	40
1/4	35	145	1/2	20	40
1/2	72	145	1/1	40	40
1/1	145	145			

4.2.1 Concentration ratio's of Copper and Nickel

4.2.1.1 Binary metal mixture of 5,4 mg/L copper and 145 mg/L nickel

In figure 46 the breakthrough curve of 5,4 mg/L copper and 145 mg/L nickel as a function of time are presented.

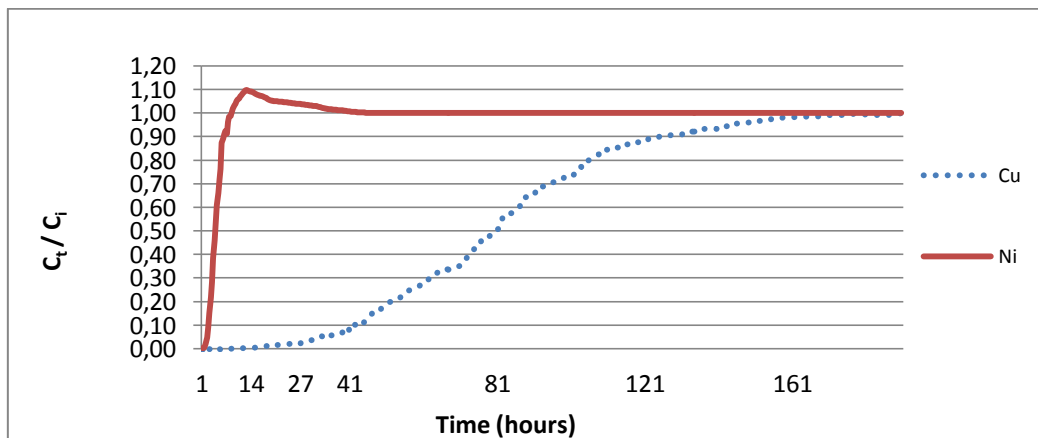


Figure 46: Breakthrough curve of copper and nickel with a full column (conditions: $C_{i, cu} = 5,78$ mg/L; $C_{i, ni} = 155$ mg/L; column length = 7 cm; flow rate = 30 ml/hour)

As can be seen in the figure above, copper is totally sorbed for several hours while nickel is not. The figure shows a nice overshoot of nickel and copper has a S-shape.

The initial concentration is reached for both metals after 170 hours. After analysing the results it can be said that the nickel ions can be separated from the mixture during 14 hours that corresponds to a separation volume of 1,07 L.

4.2.1.2 Binary metal mixture of 14,5 mg/L copper and 145 mg/L nickel

In figure 47 the breakthrough curves of 14,5 mg/L copper and 145 mg/L nickel as a function of time are presented.

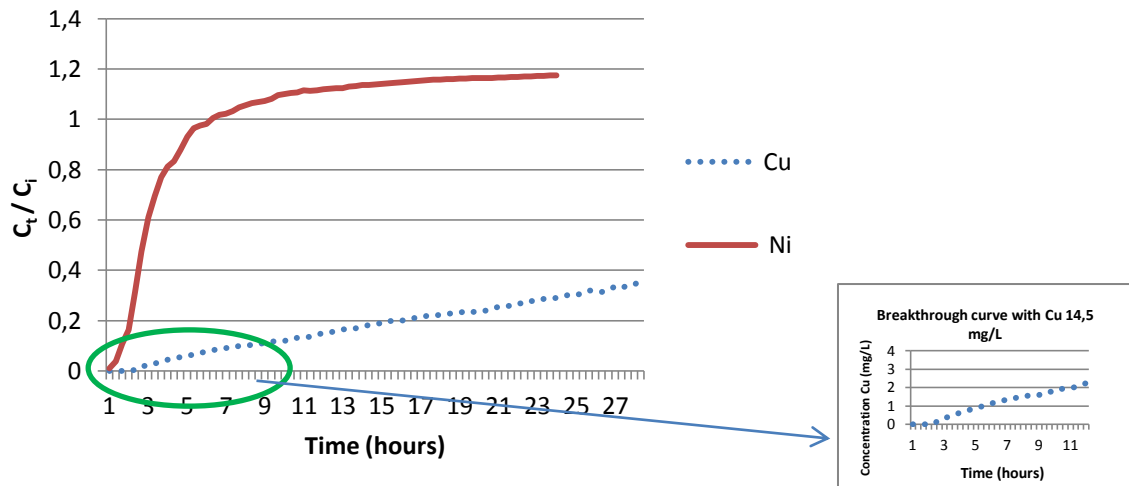


Figure 47: Breakthrough curve of 14,5 mg/L copper in a binary mixture of copper and nickel (conditions: $C_{i, Cu} = 14,92$ mg/L; $C_{i, Ni} = 145,84$ mg/L; column length = 7 cm; flow rate = 30 ml/hour)

As can be seen in the little figure, the initial concentration of copper during the first 5 hours is lower than 1 mg/L while nickel is not totally sorbed. there is separation for a few hours. The separation time is 5,5 hours and 0,14 L of solution has passed through the fixed bed.

4.2.1.3 Binary metal mixture of 35 mg/L copper and 145 mg/L nickel

In figure 48 the breakthrough curves of 35 mg/L copper and 145 mg/L nickel as a function of time are presented.

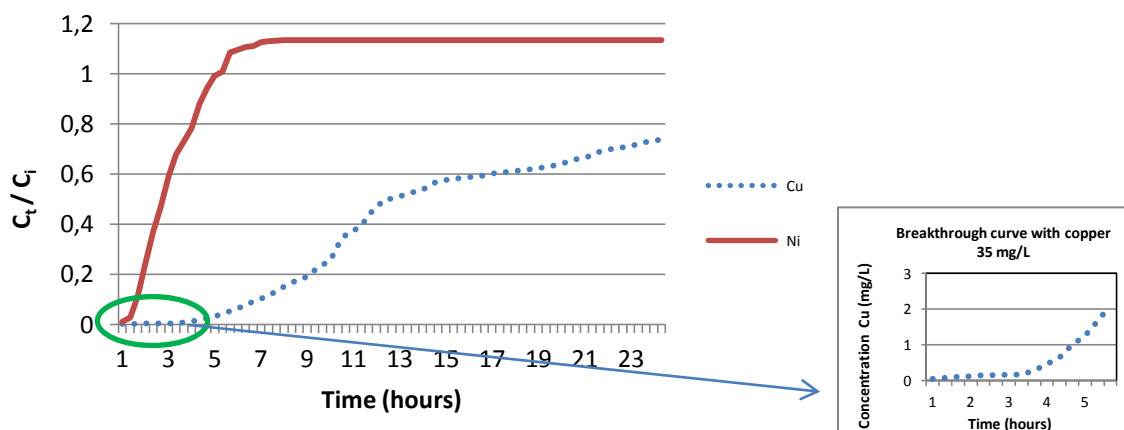


Figure 48: Breakthrough curve of 35 mg/L copper in a binary mixture of copper and nickel (conditions: $C_{i, cu} = 38,84 \text{ mg/L}$; $C_{i, ni} = 142,77 \text{ mg/L}$; column length = 7 cm; flow rate = 30 ml/hour)

As can be seen in the little figure next to figure 48, the initial concentration of copper during the first 4,5 hours is lower than 1 mg/L while nickel is not totally sorbed. There is separation for a few hours between copper and nickel. Nickel is separated from copper for 4,5 hours and 0,12 L of solution has passed through the fixed bed.

4.2.1.4 Binary metal mixture of 72,5 mg/L copper and 145 mg/L nickel

In figure 49 the breakthrough curves of 72,5 mg/L copper and 145 mg/L nickel as a function of time are presented.

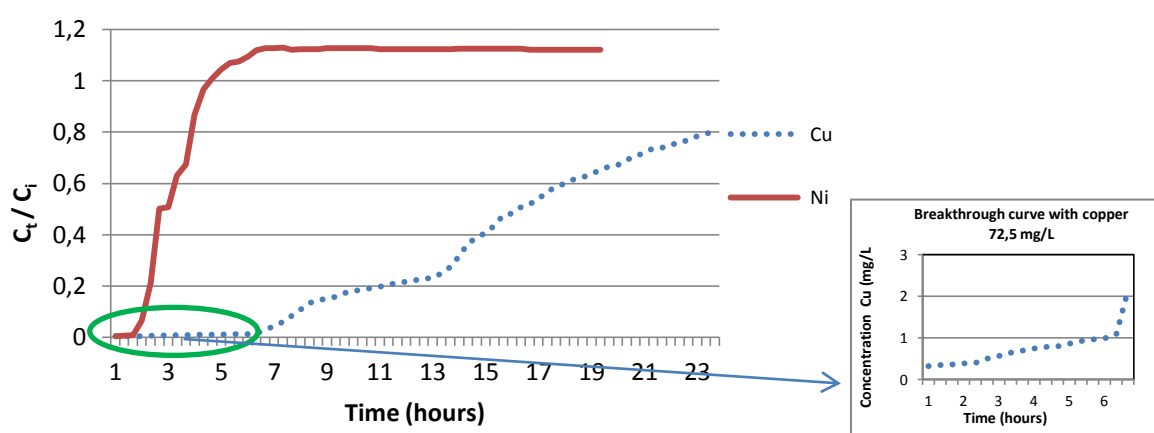


Figure 49: Breakthrough curve of 72,5 mg/L copper in a binary mixture of copper and nickel (conditions: $C_{i, cu} = 74,55 \text{ mg/L}$; $C_{i, ni} = 154,12 \text{ mg/L}$; column length = 7 cm; flow rate = 30 ml/hour)

In figure 49 it can be seen that there is separation for 6 hours when and 0,16 L passed through the column during the separation. Copper was never totally removed. This could be due to the saturation of the grape stalks for the nickel ions that are bound onto the grape stalks and prevent that all copper ions can be sorbed in the beginning. So some of the copper ions cannot be sorbed and emerge out the column.

4.2.1.5 Binary metal mixture of 145 mg/L copper and 145 mg/L nickel

In figure 50 the breakthrough curve of 145 mg/L copper and 145 mg/L nickel as a function of time are presented.

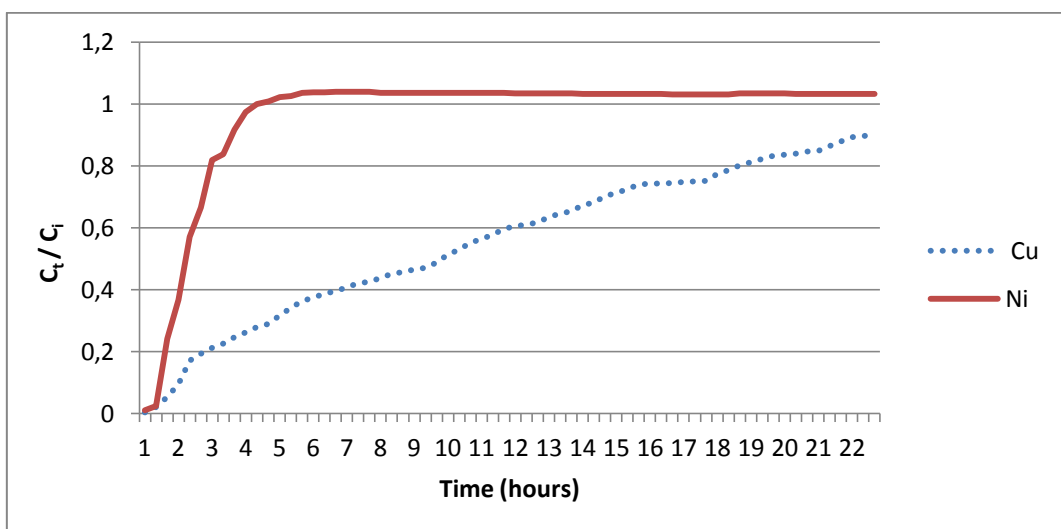


Figure 50: Breakthrough curve of 145 mg/L copper in a binary mixture of copper and nickel (conditions: $C_{i, cu} = 153,24$ mg/L; $C_{i, ni} = 158,14$ mg/L; column length = 7 cm; flow rate = 30 ml/hour)

As can be seen in figure 50 the concentration of nickel and copper increases immediately. There is no separation. The concentration of copper is too high to obtain separation with the conditions used.

In the table below the summary of the results from the different concentration of the binary metal mixture of copper and nickel are presented.

Table 8: Summary of the separation volume of the binary metal mixture as a function of copper concentration at a fixed nickel concentration of 145 mg/L

Concentration of copper (mg/L)	Separation time (hours)	separation volume (L)
5,4	14	1,07
14,5	5,5	0,14
35	4,5	0,12
72,5	6	0,16
145	0	0

From these results it can be concluded that for a fixed nickel concentration, when the concentration of copper increases from 5,4 mg/L to 14,5 mg/L, the separation time decreases. It seems that when the initial concentration of copper is 14,5 mg/L, 35 mg/L or 72,5 mg/L, at a fixed nickel concentration of 145 mg/L is used, the separation time is almost similar. This could be due to the high concentration of nickel that saturate the active site of the sorbent during the first hour and does not permit that all copper ions can be adsorbed from the solution.

4.2.1.6 Relationship between the separation volume and the initial concentration of copper

In the figure below the relationship between the separation volume and the initial concentration of copper is presented.

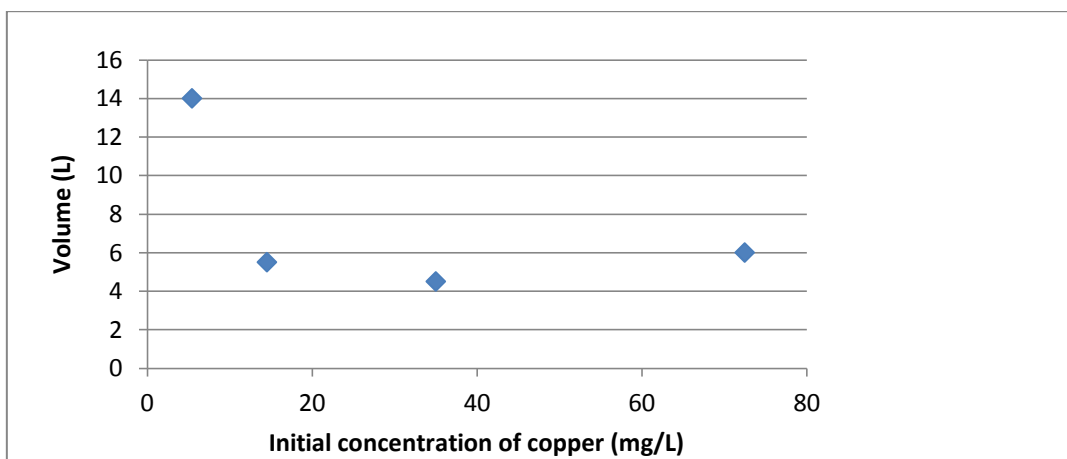


Figure 51: Relationship between the separation volume and the initial concentration of copper

There is no linear tendency in the figure presented above. There is no relationship between the separation volume and the initial concentration of copper.

4.2.2 Concentration ratio's of lead and cadmium

4.2.2.1 Binary metal mixture of 3 mg/L lead and 40 mg/L cadmium

In figure 52 the breakthrough curve of 3 mg/L lead and 40 mg/L cadmium in function of time are presented.

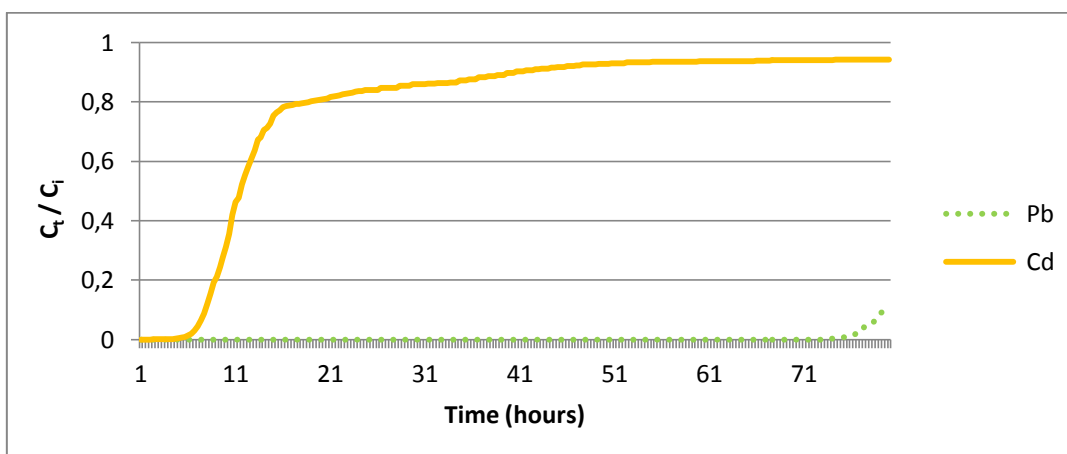


Figure 52: Breakthrough curve of 3 mg/L lead in a binary mixture of lead and cadmium (conditions: $C_{i, Pb} = 3,18$ mg/L; $C_{i, Cd} = 42,68$ mg/L; column length = 7 cm; flow rate = 30 ml/hour)

A nice S-curve is visible for cadmium as can be seen in the figure above. The first two hours no metal is measured in the outflow solution, thus both metals are totally sorbed by the grape stalks. Cadmium is separated from lead for 73 hours or for 2,18 litres of initial metal mixture solution.

4.2.2.2 Binary metal mixture of 9 mg/L lead and 40 mg/L cadmium

In figure 53 the breakthrough curve of 9 mg/L lead and 40 mg/L cadmium are presented in function of time.

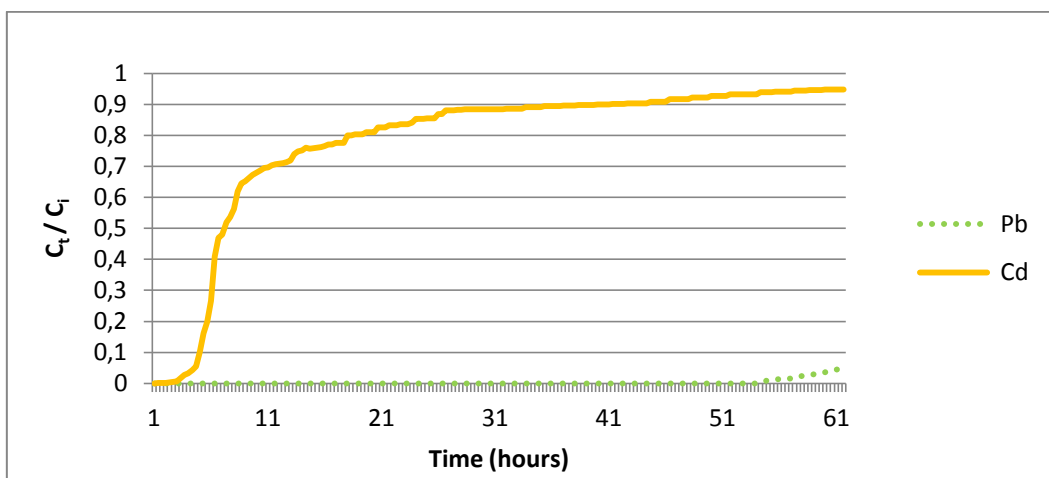


Figure 53: Breakthrough curve of 9 mg/L lead in a binary mixture of lead and cadmium (conditions: $C_{i, Pb} = 8,88 \text{ mg/L}$; $C_{i, Cd} = 41,68 \text{ mg/L}$; column length = 7 cm; flow rate = 30 ml/hour)

The big separation time is clearly visible on the figure above. The separation is lasting for 54 hours and 1,6 litres of solution goes through the column when separation takes place.

4.2.2.3 Binary metal mixture of 20 mg/L lead and 40 mg/L cadmium

In figure 54 the breakthrough curve of 20 mg/L lead and 40 mg/L cadmium are presented in function of time.

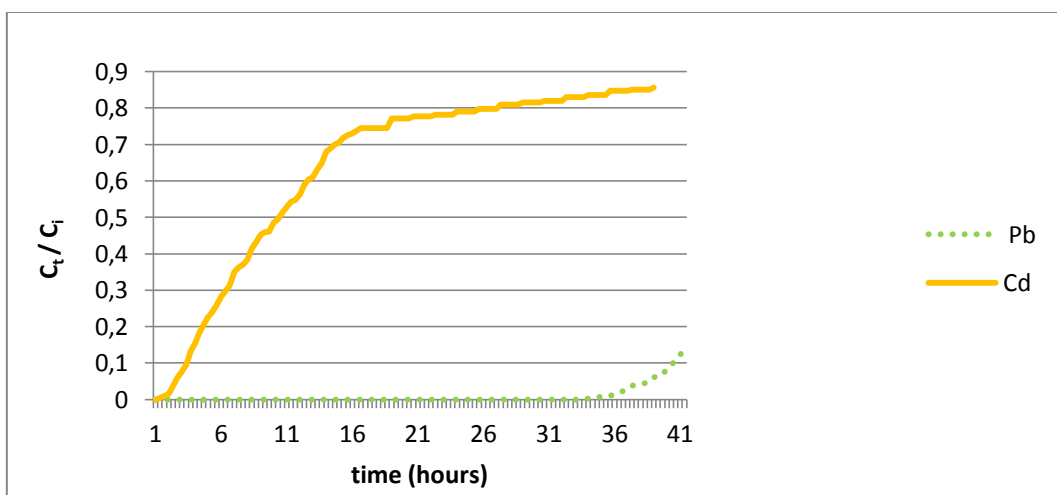


Figure 54: Breakthrough curve of 20 mg/L lead in a binary mixture of lead and cadmium (conditions: $C_{i, Pb} = 18,24 \text{ mg/L}$; $C_{i, Cd} = 42,05 \text{ mg/L}$; column length = 7 cm; flow rate = 30 ml/hour)

As can clearly be seen in the figure above there is separation between both metals. Cadmium ions are separated from lead for 33 hours or for 0,98 litres of initial metal mixture solution.

4.2.2.4 Binary metal mixture of 40 mg/L lead and 40 mg/L cadmium

In figure 55 the breakthrough curve of 40 mg/L lead and 40 mg/L cadmium are presented in function of time.

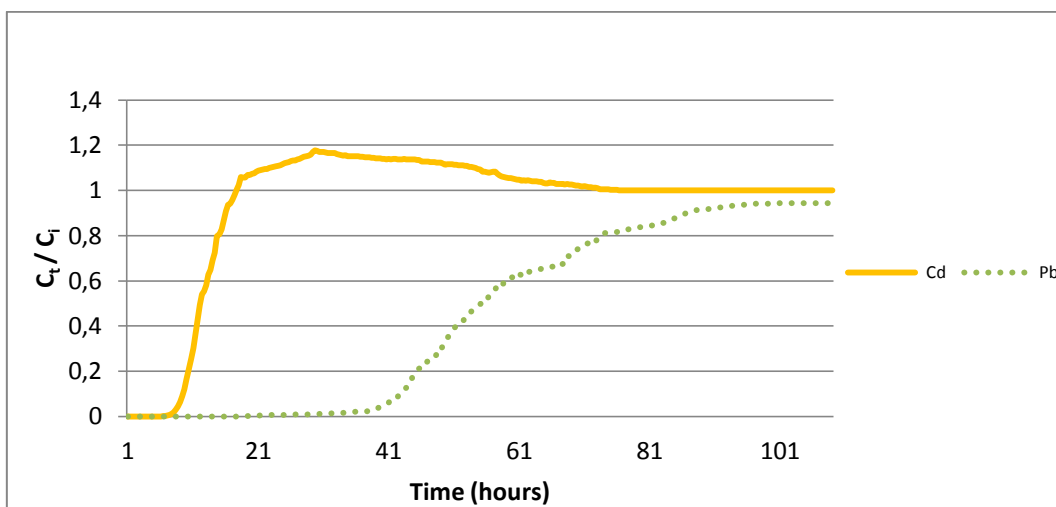


Figure 55: Breakthrough curve of Pb and Cd with a full column (conditions: $C_{i, Pb} = 40,38 \text{ mg/L}$; $C_{i, Cd} = 47,67 \text{ mg/L}$; column length = 7 cm; flow rate = 30 ml/hour)

In figure 55 it can be seen that there is separation. The separation is lasting for 10 hours and 0,42 litres of solution goes through the column when separation takes place. The first five hours both cadmium and lead are totally sorbed.

In the table below the summary of the results from the different concentration ranges of the binary metal mixture of lead and cadmium are presented.

Table 9: Summary of the concentration ranges of the binary metal mixture of lead and cadmium

Concentration of lead (mg/L)	Separation time (hours)	separation volume (L)
40	10	0,42
20	33	0,98
9	54	1,6
3	73	2,18

As can be seen in the table above cadmium can be separated from lead for all experiments. When the lead concentration decreases or the concentration ratio between lead and cadmium increases, then the separation time also increases as so the amount of separation volume used during the separation.

4.2.2.5 Relationship between the separation volume and the initial concentration of lead

In the figure below the relationship between the separation volume and the initial concentration of lead is presented.

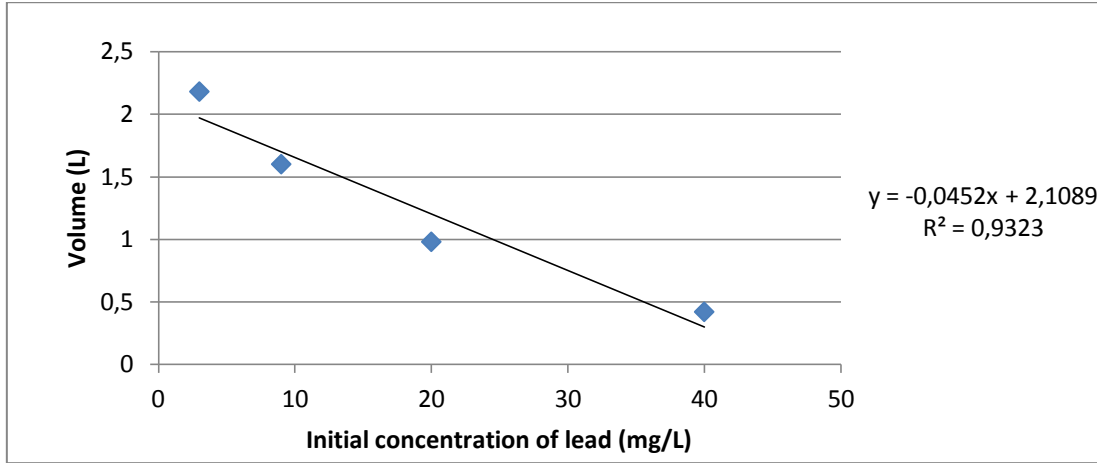


Figure 56: Relationship between the separation volume and the initial concentration of lead

The higher the initial concentration of lead increases in the binary metal mixture of cadmium and lead, the less volume of cadmium solution is separated. There is a good linear relationship visible.

4.3 BED-DEPTH SERVICE TIME MODEL (BDST)

The BDST model offers the simplest approach and rapid prediction of the adsorber design and performance. The BDST is a model for predicting the relationship between bed depths, X and service time t . A linear relationship between bed-depth and service time may be given by the equation:

$$t = \frac{N_0}{vC_0}X - \frac{1}{KC_0} \ln \left(\frac{C_0}{C_b} - 1 \right)$$

with:

t = the service time of the column (hours)

N_0 = maximum adsorption capacity (mg/L)

v = the linear flow velocity of feed to bed (cm/hours)

C_0 = the initial concentration of solute (mg/L)

X = the bed depth of column (cm)

K = the adsorption rate constant (L/mg.hours)

C_b = the desired concentration of solute at breakthrough (mg/L)

From the equation above the service time can be predicted for different concentration levels of metals in different bed lengths. N_0 and K can be evaluated from slope (a) and the intercept (b) of the plot of service time versus the bed depth, respectively. (Negrea et al., 2011)

$$(a) \ a = \frac{N_0}{vC_0}$$

$$(b) \ b = \frac{1}{KC_0} \ln \left(\frac{C_0}{C_b} - 1 \right)$$

4.3.1 Relationship between the separation time and the bed length for the binary metal mixture of copper and nickel

In the figure below the relationship between the separation time and the bed length of the metal mixture of copper 4,5 mg/L and nickel 145 mg/L is presented.

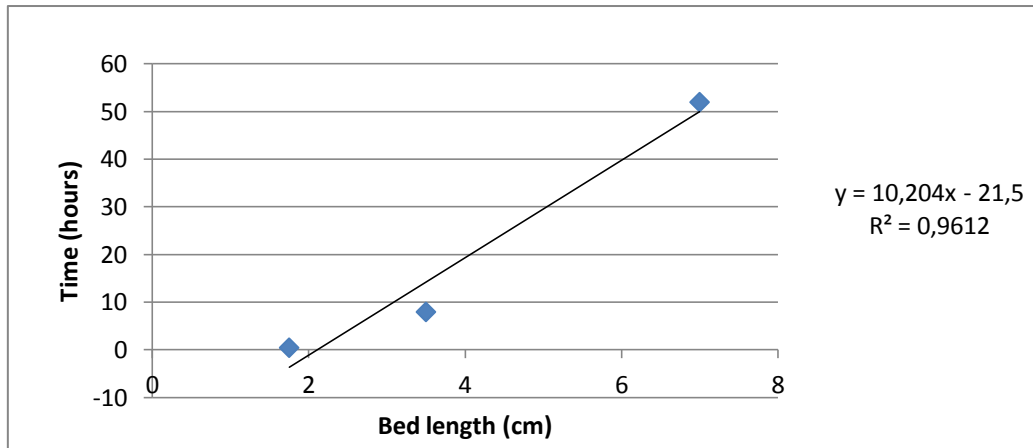


Figure 57: Relationship between the separation time and the bed length of the binary metal mixture of copper and nickel

There is a linear relationship visible in the figure above. When the bed length increases in a binary metal mixture of copper and nickel, then the separation time also increases. The equation obtained in the figure above is used to find BDST's for different concentrations of copper and different bed lengths.

Table 10 presents the values N_0 and K for copper. These values are used in the equation to predict the BDST.

Table 10: N_0 and K values for copper

metal	N_0 (mg/L)	K (L/(mg.hours))
Cu	2104,88	0,0128

The table below presents the prediction of the BDST for the binary metal mixture of copper and nickel for different copper concentrations with a fixed nickel concentration of 145 mg/L.

Table 11: Prediction of the BDST for the metal mixture of copper/nickel for different copper concentrations

Copper concentration in mg/L	5,4	14,5	35	72,5	145
Prediction of the BDST for a full column	50 hours	12,5 hours	3 hours	1 hours	0 hours
BDST of the results in this work for a full column	52 hours	5 hours	4,5 hours	6 hours	0,5 hours

The BDST model cannot be used to predict the separation time as a function of the concentration for copper and nickel by the experimental conditions used in this work.

The BDST's predicted don't match the BDST's found in this work for all copper concentrations higher than 5,4 mg/L. This model cannot be used because when the initial concentration of copper is 14,5 mg/L, 35 mg/L or 72,5 mg/L, at a fixed nickel concentration of 145 mg/L, the separation time is almost similar probably due to the high concentration of nickel.

Table 12: Prediction of the BDST for the metal mixture of copper 5,4 mg/L and nickel 145 mg/L for different bed lengths

Bed length	1,75 cm	3,5 cm	7 cm	15 cm	30 cm	50 cm
Prediction of the BDST with a copper concentration of 5,4 mg/L and a nickel concentration of 145 mg/L	0 hours	14 hours	50 hours	133,5 hours	284,5 hours	488,5 hours
BDST of the results in this work for a copper concentration of 5,4 mg/L and a nickel concentration of 145 mg/L	0 hours	8 hours	52 hours			

As can be seen in the table above, the results predicted by the model are similar to the experimental values. The BDST model can be used to predict the separation time as a function of the bed depth for the metal mixture of copper and nickel by the experimental conditions used in this work. The separation volume for every bed depth for copper 4,5 mg/L and nickel 145 mg/L can be predicted by using the equation of the BDST model. In the table above the BDST is predicted for bed depths higher than 7 cm.

4.3.2 Relationship between the separation time and the bed length for the binary metal mixture of cadmium and lead

The table below presents the relationship between the separation time and the bed length of the binary metal mixture of lead and cadmium.

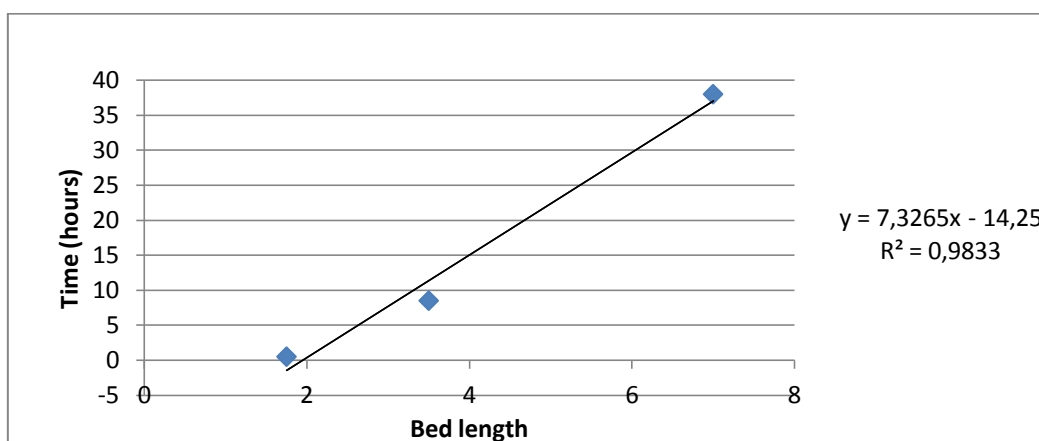


Figure 58: Relationship between the separation time and the bed length of the binary metal mixture of lead and cadmium

Figure 58 presents a linear tendency of the relationship between the separation time and the bed length of the binary metal mixture of lead 45 mg/L and cadmium 52 mg/L. The equation in the figure above is used to find the BDST.

Table 13 presents the values N_0 and K for lead. These values are used in the equation to predict the BDST.

Table 13: N_0 and K values for lead

metal	N_0 (mg/L)	K (L/mg.hours)
Pb	11195	0,00643

The tables below presents the prediction of the BDST for the binary metal mixture of lead and cadmium for different lead concentrations with a fixed cadmium concentration of 52 mg/L.

Table 14: Prediction of the BDST for the metal mixture of lead/cadmium for different lead concentrations

Lead concentration in mg/L	40	20	9	3
Prediction of the BDST for a full column with a fixed cadmium concentration	37 hours	84 hours	209 hours	734 hours
BDST of the results in this work for a full column with a fixed cadmium concentration	38,5 hours			

The BDST model cannot be used to predict the separation time as a function of the concentration for lead and cadmium by the experimental conditions used in this work. Only with a lead concentration of 40 mg/L can the predicted BDST be compared with the experimental results. The experimental results of the BDST for lead concentrations lower than 40 mg/L are not conducted and thus cannot be compared.

Table 15: Prediction of the BDST for the metal mixture of lead 45 mg/L and cadmium 52 mg/L for different bed lengths.

Bed length	1,75 cm	3,5 cm	7 cm	15 cm	30 cm	50 cm
Prediction of the BDST for a lead concentration of 40 mg/L and a cadmium concentration of 52 mg/L	0 hours	11,5 hours	37 hours	95,5 hours	205,5 hours	352 hours
BDST of the results in this work for a lead concentration of 40 mg/L and a cadmium concentration of 52 mg/L	0,5 hours	8 hours	38,5 hours			

As can be seen in the table above, the results predicted by the model are similar to the experimental values. The BDST model can be used to predict the separation time as a function of the bed depth for the metal mixture of lead and cadmium by the experimental conditions used in this work. The separation volume for every bed depth can be predicted by using the equation of the BDST model. In the table above the BDST is predicted for bed depths higher than 7 cm.

5 **CONCLUSIONS**

After studying the separation of two binary metal mixtures by using grape stalks, the following conclusions were drawn:

- By using optimal conditions, fixed columns filled with grape stalks are an effective method to separate metals in a binary metal mixture solution of copper and nickel and a binary metal mixture solution of cadmium and lead. Copper is removed from the solution while nickel stays in the solution. Lead is removed from the solution while cadmium remains in the solution.
- Separation volume of the binary metal mixtures depends on the bed lengths. When the bed length increases, the separation time also increases. A minimum bed length was necessary to achieve separation. The minimum bed length depends on the metals in the mixture solution and the concentration of both metals in the mixture.
- The metal concentration affects the separation volume. In the binary metal mixture of cadmium with a fixed concentration of 52 mg/L and a lower concentration of lead, a decrease of the lead concentration results in an increase of separation volume. However, in the case of a fixed nickel concentration of 145 mg/L and a lower copper concentration, the increase of separation volume when copper concentration decreases is not observed. This could be due to the high content of nickel ions that saturates the active sites of the sorbent during the first hour and does not permit that all copper ions can be adsorbed from the solution.
- The BDST model can be used to predict separation time for different bed lengths at the fixed initial concentration studied.

6 **ANNEX**

Table 16: Pump tubes color codes

ID inch	ID mm	code		color code		Ismatec order # for Tygon® ST R-3603/R-3607	standard flow rate ml/min	Ismatec IPC 1% ml/min	Ismatec IPC 100% ml/min
0.0050	0.13	-		orange-black		SC0188	-	-	-
0.0075	0.19	ENE01		orange-red		SC0001	0.048	0.004	0.24
0.0100	0.25	ENE02		orange-blue		SC0002	0.083	0.007	0.40
0.0150	0.38	ENE03		orange-green		SC0003	0.12	0.008	0.87
0.0175	0.44	ENE04		green-yellow		SC0004	0.16	0.015	1.15
0.0200	0.51	ENE05		orange-yellow		SC0005	0.21	0.023	1.52
0.0225	0.57	ENE06		white-yellow		SC0006	0.23	0.025	1.88
0.0250	0.64	ENE07		orange-white		SC0007	0.30	0.029	2.34
0.0300	0.76	ENE08		black-black		SC0008	0.38	0.040	3.25
0.0350	0.89	ENE09		orange-orange		SC0009	0.49	0.043	4.38
0.0375	0.95	ENE10		white-black		SC0010	0.60	0.06	4.95
0.0400	1.02	ENE11		white-white		SC0011	0.66	0.063	5.66
0.0430	1.09	ENE12		white-red		SC0012	0.75	0.069	6.42
0.0450	1.14	ENE13		red-red		SC0013	0.83	0.08	6.98
0.0480	1.22	ENE14		red-grey		SC0014	0.92	0.100	7.93
0.0510	1.30	ENE15		grey-grey		SC0015	1.00	0.100	8.93
0.0560	1.42	ENE16		yellow-yellow		SC0016	1.20	0.120	10.52
0.0600	1.52	ENE17		yellow-blue		SC0017	1.31	0.140	11.93
0.0650	1.65	ENE18		blue-blue		SC0018	1.58	0.150	13.88
0.0690	1.75	ENE19		blue-green		SC0019	1.81	0.190	15.46
0.0730	1.85	ENE20		green-green		SC0020	1.88	0.210	17.10
0.0810	2.06	ENE21		purple-purple		SC0021	2.44	0.230	20.77
0.0900	2.29	ENE22		purple-black		SC0022	2.88	0.280	25.09
0.1000	2.54	ENE23		purple-orange		SC0023	3.19	0.330	30.11
0.1100	2.79	ENE24		purple-white		SC0024	3.78	0.350	35.43
0.1250	3.17	-		black-white		SC0222	-	0.450	43.98

7 **BIBLIOGRAPHY**

- (2003, 4 3). *Adsorption*. R.M. Price. Retrieved from website:
<http://facstaff.cbu.edu/rprice/lectures/adsorb.html>
- Anish, T. J., Jain, N., Joshi, H. C., & Prasad, S. (2008, July 1). *Agricultural and agro-processing wastes as low cost adsorbents for metal removal from wastewaters: A review*. (Division of Environmental Sciences, Indian Agrochemical Research Institute) Retrieved June 29, 2007, from <http://nopr.niscair.res.in/bitstream/123456789/1862/1/JSIR%2067%289%29%20647-658.pdf>
- Ayora, C., Caraballo, M. A., Macias, F., Rötting, T. S., Carrera, J., & Nieto, J.-M. (2012, November 15). *Acid mine drainage in the Iberian Pyrite Belt: 2. Lessons learned from recent passive remediation experiences*. (Springer-Verlag Berlin Heidelberg 2013) Retrieved March 19, 2013
- Escudero, C., Poch, J., & Villaescusa, I. (2012). *Modelling of breakthrough curves of single and binary mixtures of Cu(II), Cd(II), Ni(II) and Pb(II) sorption onto grape stalks waste*. Universitat de Girona: Elsevier.
- Galán, E., Gómez-Ariza, J. L., González, I., Caliani-Fernández, J. C., Morales, E., & Giráldez, I. (2001, July 15). *Heavy metal partitioning in river sediments severely polluted by acid mine drainage in the Iberian Pyrite Belt*. (Pergamon) Retrieved March 15, 2002, from http://www.researchgate.net/profile/Juan_Fernandez-Caliani/publication/223753368_Long-term_interaction_of_wollastonite_with_acid_mine_water_and_effects_on_arsenic_and_metal_removal/links/0deec5178d0555f3d0000000.pdf
- José, N. M., Aguasanta, S. M., Manuel, O., Carlos, C. R., Inmaculada, R., Judit, K., & T., D. A. (2006). *Acid mine drainage pollution in the Tinto and Odiel rivers (Iberian Pyrite Belt, SW Spain) and bioavailability of the transported metals to the Huelva Estuary*. Spain: Elsevier. Retrieved from <https://www.mendeley.com/viewer/?fileId=78aa1aa7-218e-8221-41a6-60586ceac34a&documentId=488fe32e-4af3-35fc-9116-2795bbd4b274>
- Negrea, A., Ciupac, M., Lupa, L., & Negrea, P. (2011). *Experimental and modelling studies on As(III) removal from aqueous medium on fixed bed column*. Timisoara, Romania, 2 Piata Victoriei, 300006: Universiteit Timisoara.
- Nieto, J. M., Sarmiento, M. A., Canovas, C. R., Olias, M., & Ayora, C. (2013). *Acid mine drainage in the Iberian Pyrite Belt: 1. Hydrochemical characteristics and pollutant load of the Tinto and Odiel rivers*. Berlin: Springer-Verlag.
- Oñate, C. E. (2009). *Valorisation of industrial wastes for the removal of metals and arsenic from aqueous effluents*. Girona: Universitat de Girona.
- Pujol, D., Liu, C., Fiol, N., Àngels, O. M., Gominho, J., Villaescusa, I., & Pereira, H. (2013, May 22). *Chemical characterization of different granulometric fractions of grape stalks waste*. (Elsevier) Retrieved July 21, 2013, from file:///C:/Users/Bas/Downloads/INDCRO6805.pdf
- Seader, J. (2002). *Adsorption*. R.M. Price.
- Senese, F. (2015, 08 17). *What is cellulose*. Retrieved from General chemistry online: <http://antoine.frostburg.edu/chem/senese/101/consumer/faq/what-is-cellulose.shtml>
- Sweeney, D. (1992). *What is Acid Mine Drainage*. Retrieved from <http://www.sosbluewater.org/epa-what-is-acid-mine-drainage%5B1%5D.pdf>
- Volesky, B. (2003). *Sorption and biosorption*. Montreal- ST; Lambert, Quebec, Canada: BV Sorbex, Inc.